Direct-Detection Survey Spectroscopy with CCAT

C. M. Bradford

May 13, 2008

Topics

- Scientific motivation for terrestrial submillimeter spectroscopy.
- Sensitivities of CCAT for spectroscopy, context with ALMA & pending flight opportunities.
- C+ science and high-z survey outline:
    - areal and redshift density of sources accessible to CCAT.
- Optimal spectrometer choices, relationships to present-day instruments.

Spitzer GOODS - 24 mm; Daddi et al.

Introduction: IR astronomy is **far**-IR astronomy

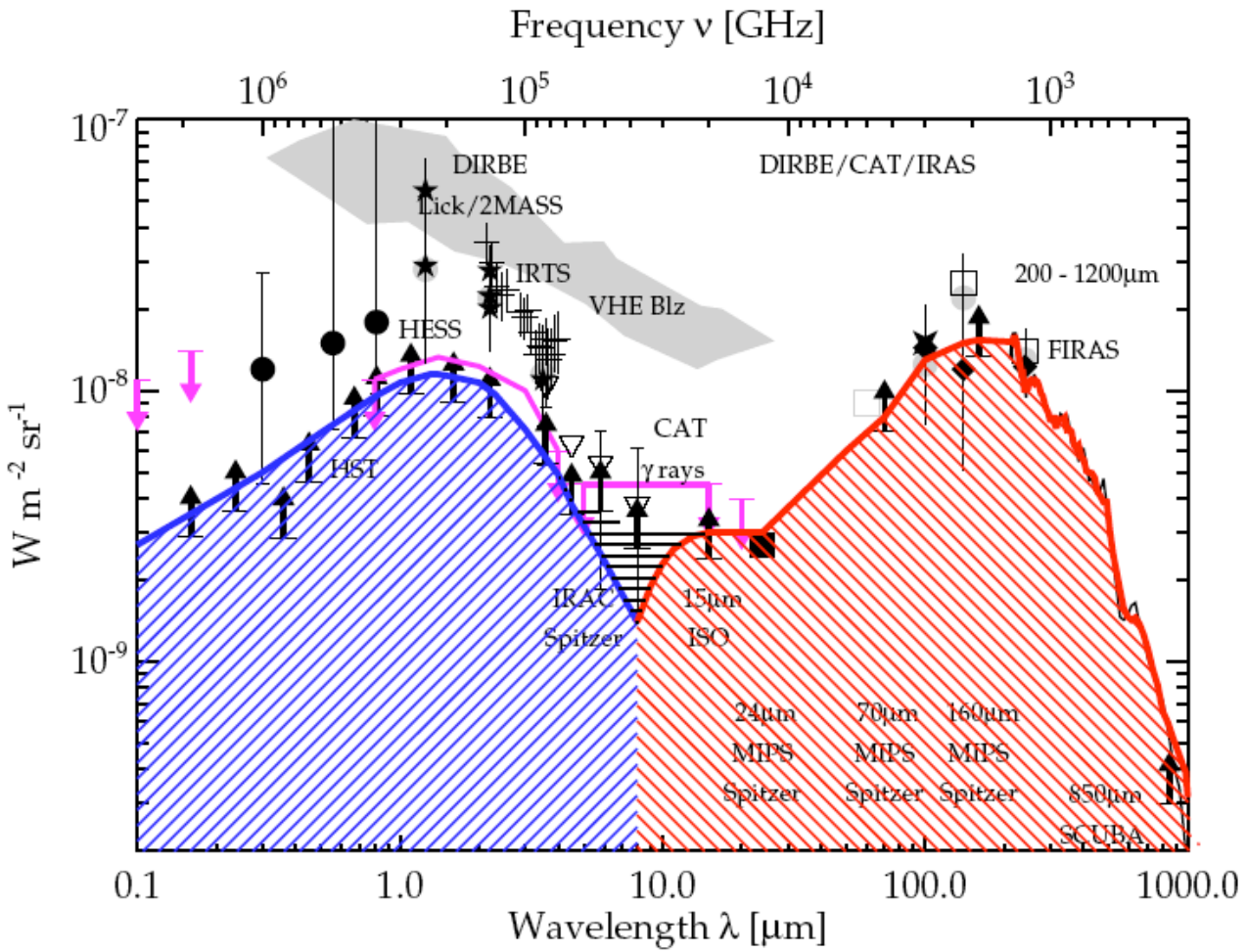

Fig. 13. Our best Cosmic Optical Background (blue-shaded, left) and Cosmic Infrared Background (red-shaded, right) estimates. The gray-shaded area represents the region of overlap. See Fig. 9 for the other symbols.

Cosmic Backgrounds
Galaxy counts + COBE + Spitzer
(Dole et al. 2005)

- History of stars and galaxies written at both optical / NIR and far-IR wavelengths.

Questions:

What have we learned about the production of the CFIRB?

What is the relationship between the populations producing the CFIRB and the COB?

Far-IR background is being resolved into galaxies

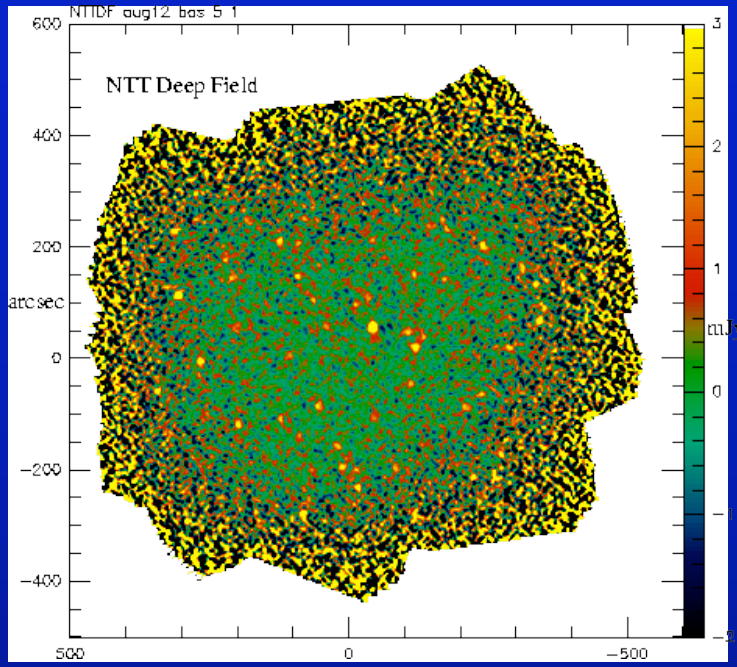

MAMBO / IRAM 30 m
1.3 mm 60 hours, 40 sources
10% of BG
Bertoldi et al. (2000);
Carilli et al. (2001c, 2002b);
Dannerbauer et al. (2002);
Voss (2002);
Eales et al. (2002)
Greve et al (2005)

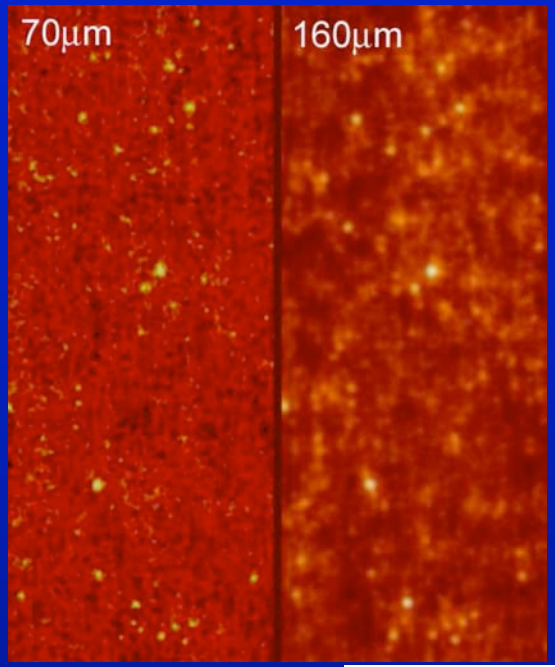

Spitzer MIPS
Chandra Deep Field South
70 (23%) 160 (7%)

Dole et al. (2004)

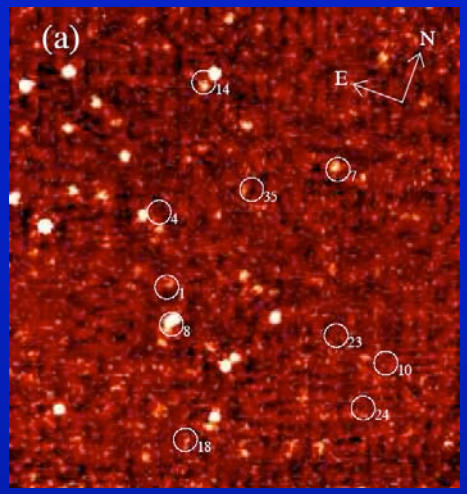

Spitzer MIPS 24 μm
Lockman Hole
Egami et al. (2004)

Dole et al. (2004)

TABLE 3
POTENTIAL RESOLUTION OF THE COSMIC INFRARED BACKGROUND

	24 μm[a]	70 μm[a]	160 μm[a]
Spitzer	74%	59%	18%
Herschel[b]/SPICA	98%	93%	58%
JWST[b]	99%	–	–
SAFIR	100%	99%	94%

NOTE. — (a) Using the CIB value from Lagache et al. (2004) and using the limiting flux using the SDC limit and assuming confusion-limited surveys. (b) This hypothesis might not be valid for Herschel and JWST.

CCAT at 350 μm: Similar to SAFIR at 160 μm

Future observatories will resolve the bulk of the background into individual sources, but
How to do meaningful follow up of these sources?

Submillimeter Galaxies

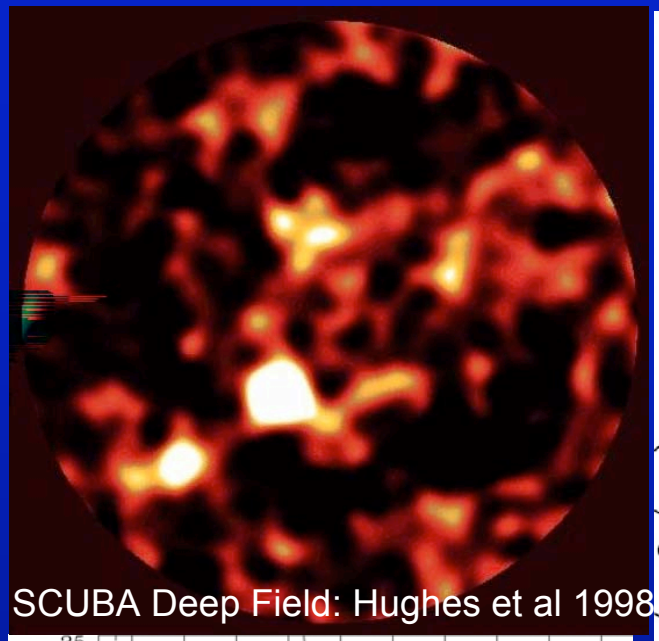

SCUBA Deep Field: Hughes et al 1998

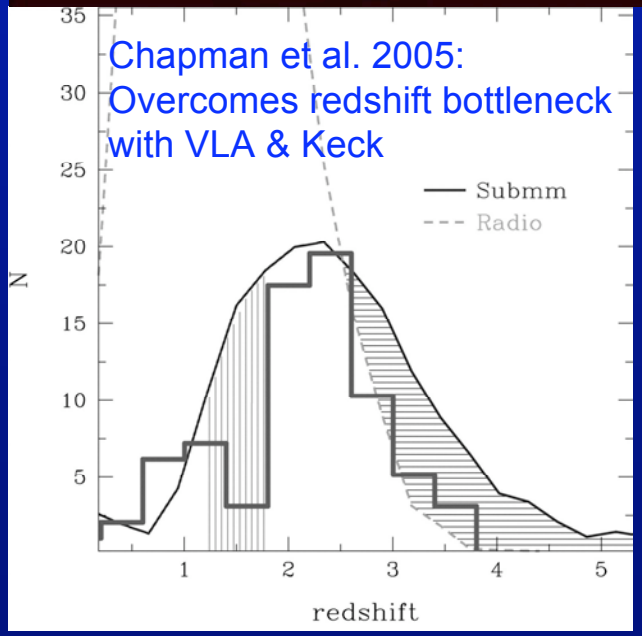

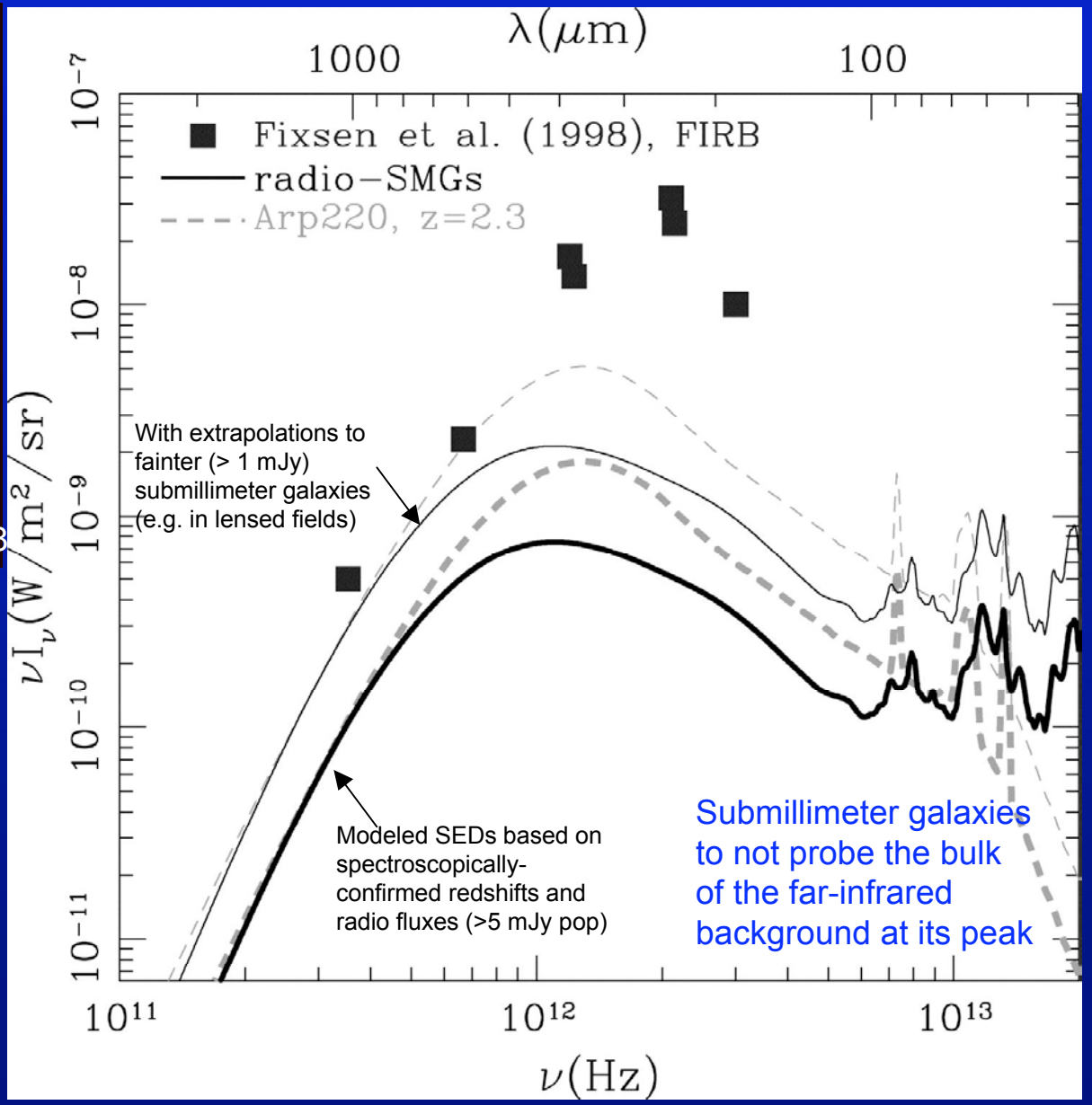

Detecting all the light at 24 microns with Spitzer MIPS

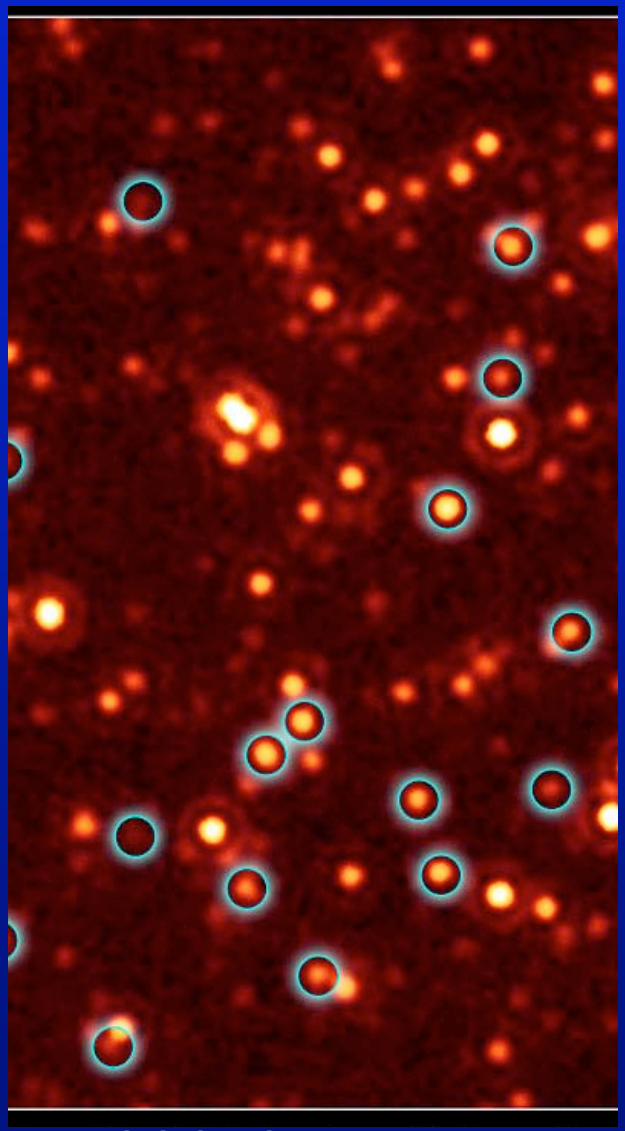

GOODS Daddi et al

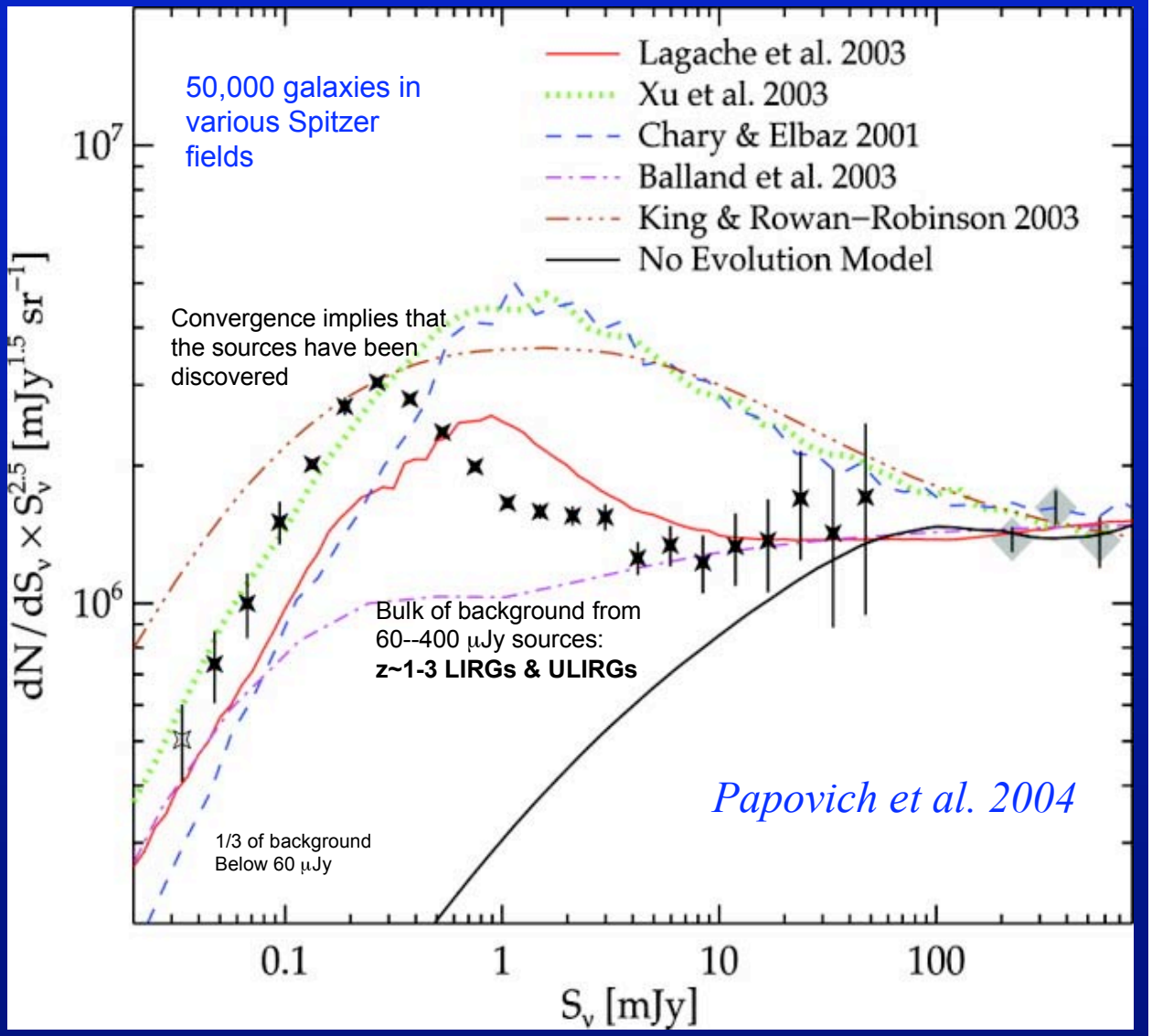

Far-IR background is largely accounted for

Dole et al. Stacking analysis based 24 on micron positions

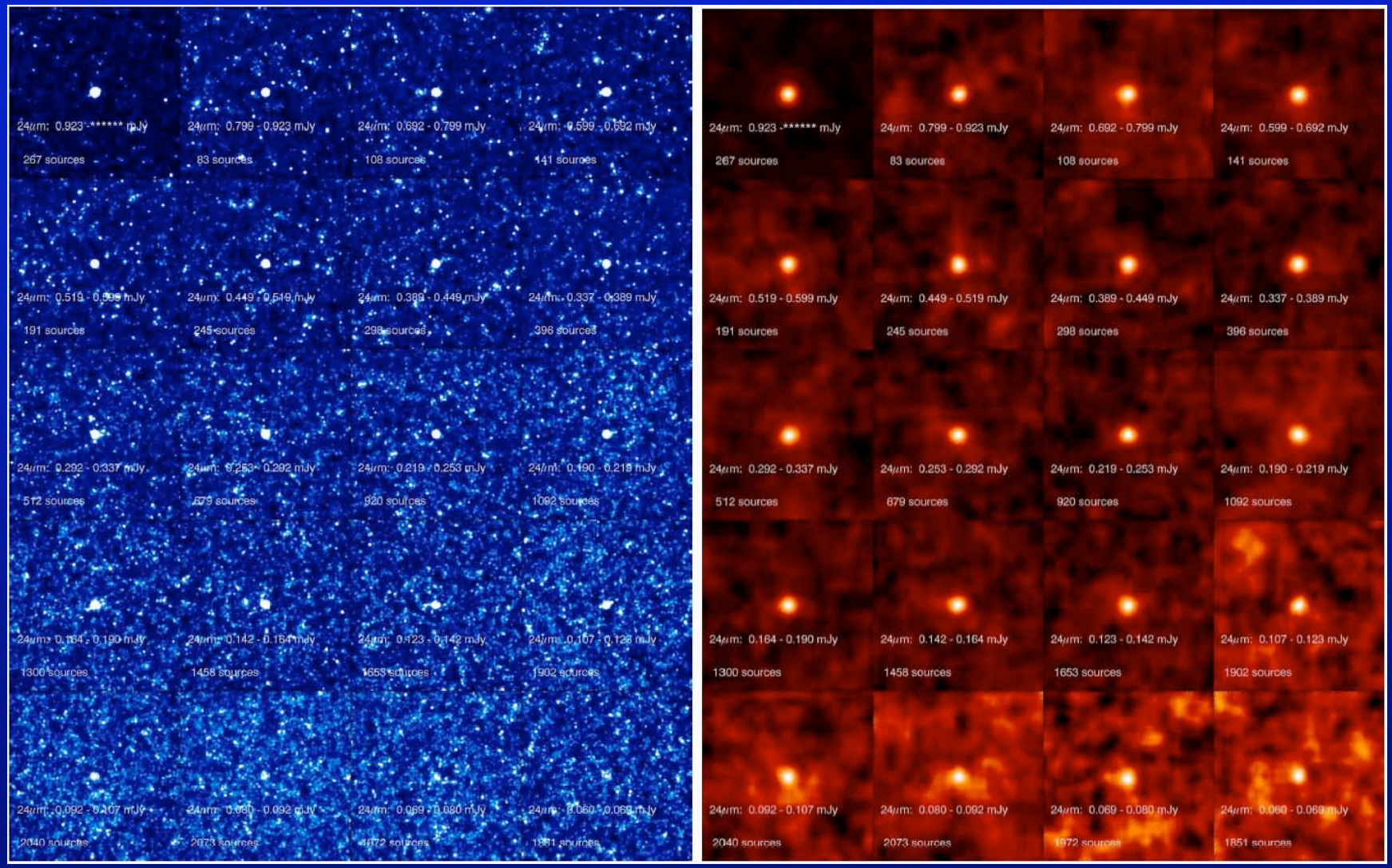

24 micron positions binned in flux

160 micron aggregate detections -- *66% of BG*

Extragalactic spectroscopy beyond 100 microns

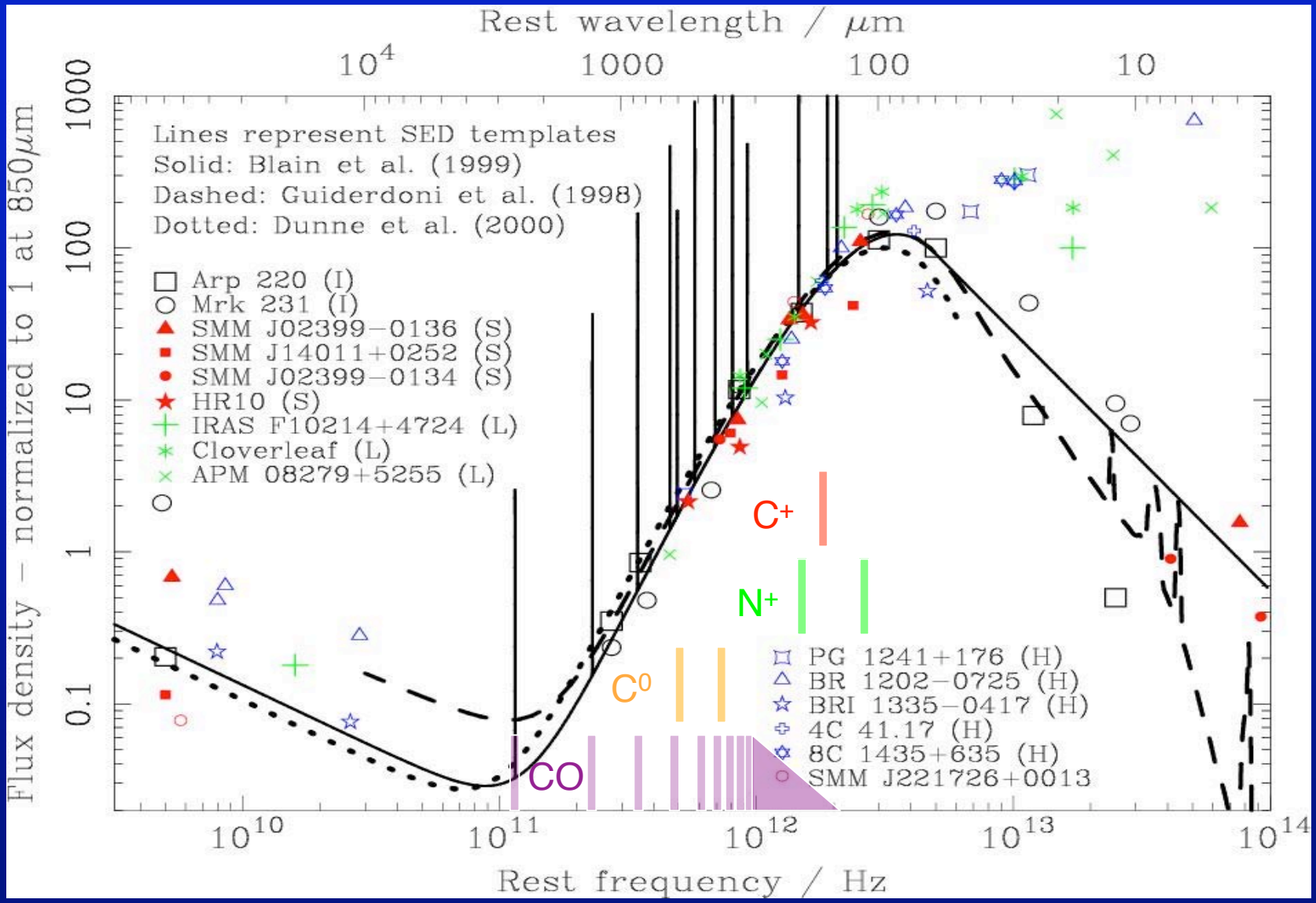

SED courtesy A. Blain

CCAT -- redshifted fine structure lines

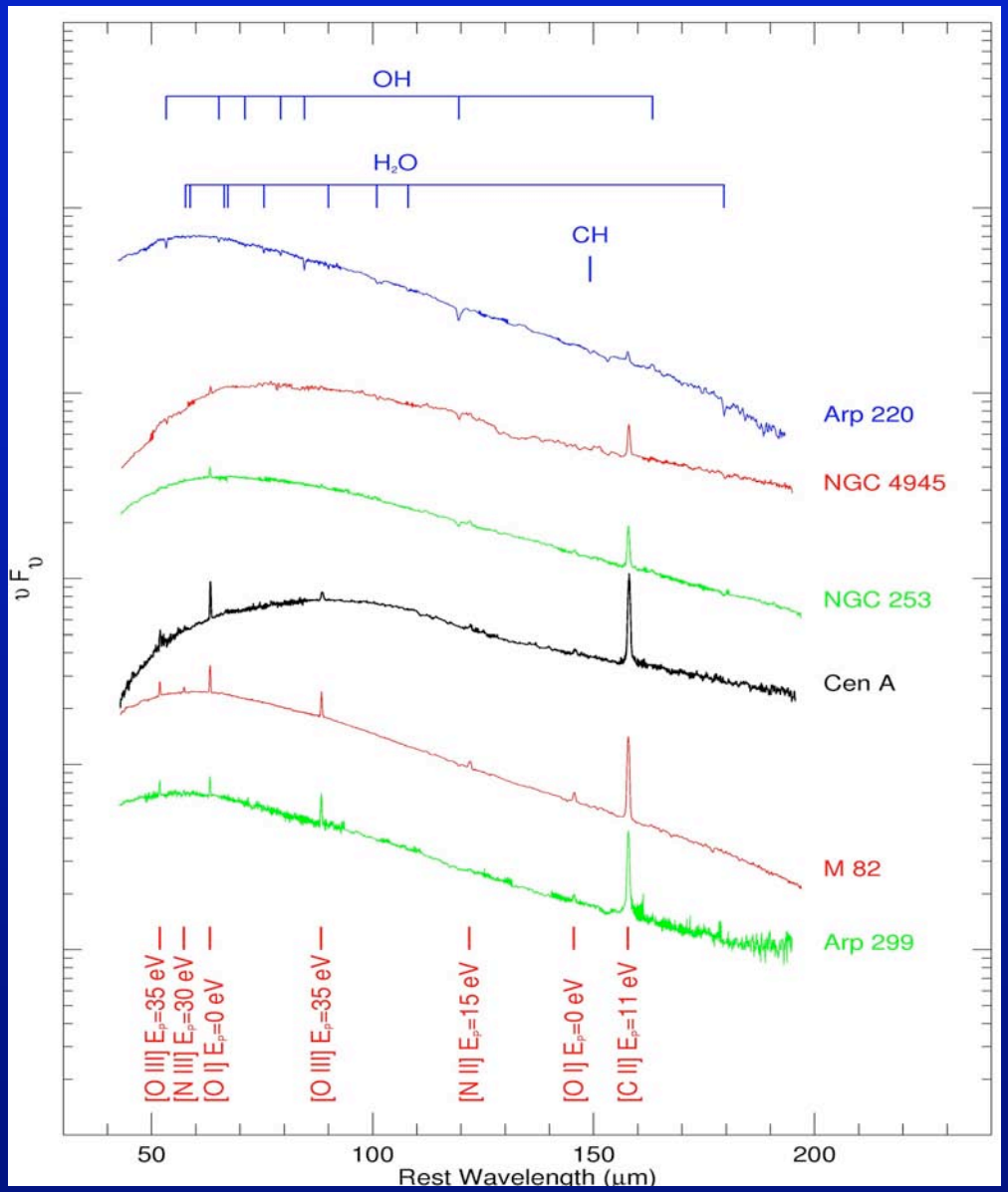

Fine structure lines probe ionized and neutral atomic gas.

- → HII region densities
- → Atomic gas pressures
- → UV field strength and hardness

→ Starburst / AGN discriminator

→ Stellar mass function

• Suite of lines is redshifted into CCAT atmospheric windows -- provides redshift template independent of optical follow-up.

-> Also provides unique, extinction-free astrophysical probes:
UV field strength, hardness
-> stellar mass function.

J. Fischer et al.1999

The Physics of the [CII] Line

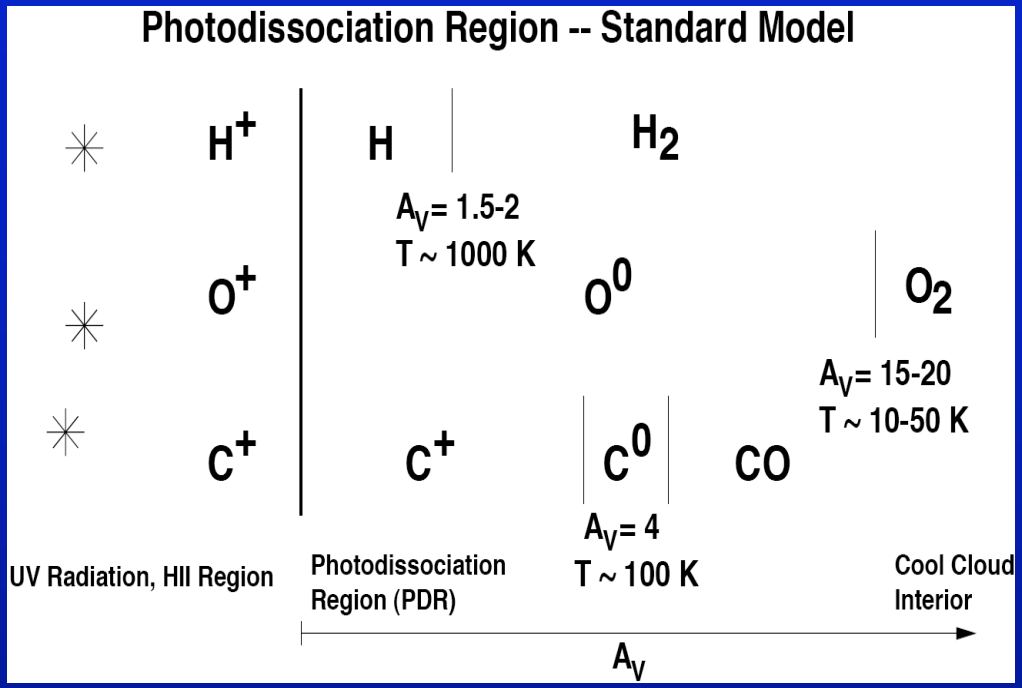

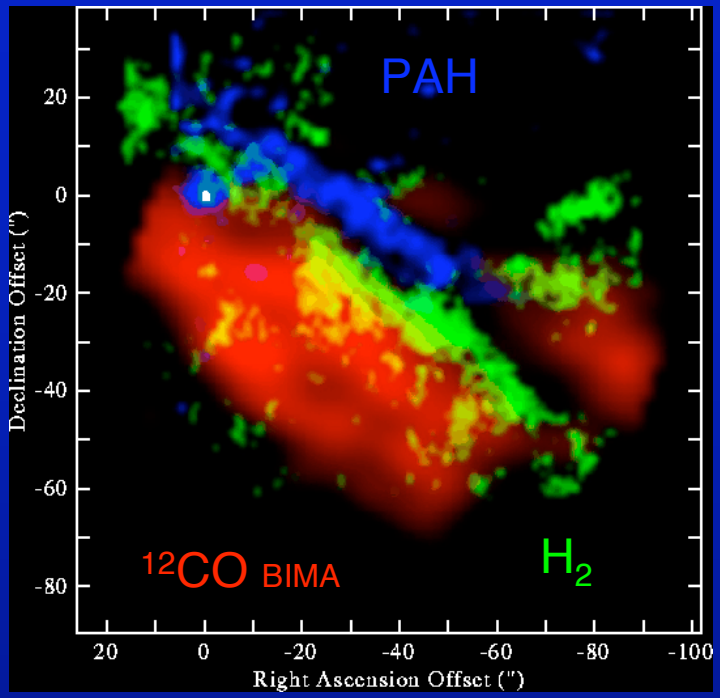

- The [CII] line arises from photodissociation regions (PDRs) on the surfaces of far-UV exposed molecular clouds
- The gas in these PDRs is heated by electrons ejected by far-UV photons: photoelectric heating
- About 1% of the far-UV photon energy goes into heating the gas. The rest goes into heating the dust which re-radiates in the far-IR continuum.
- The gas is cooled primarily by the [CII] line (important contributions from [OI] and [SiII] as well for warm, dense PDRs).

CCAT Spectroscopic Sensitivities

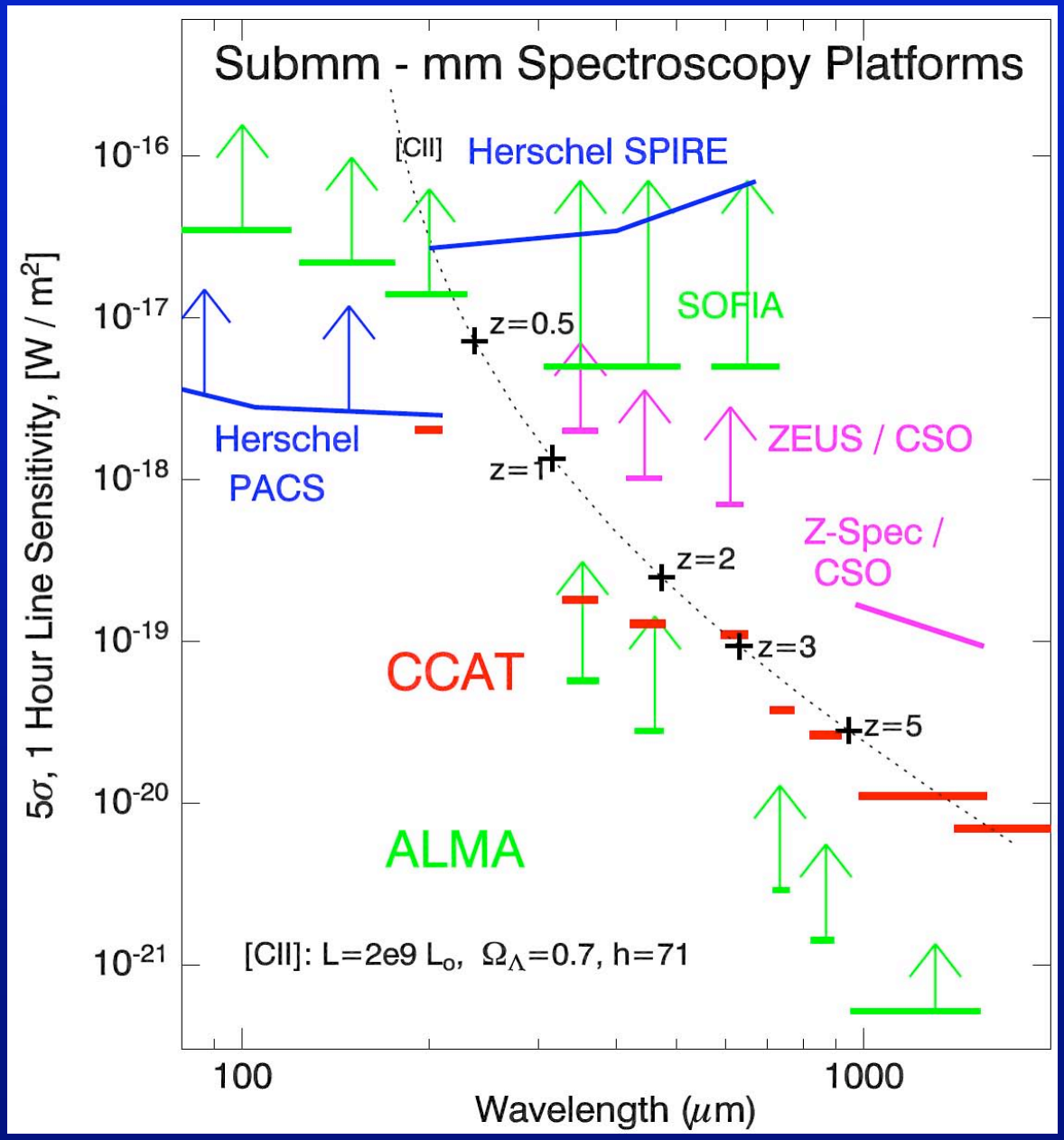

- Herschel, SOFIA -- small collecting area, no substantial advantage since warm apertures.
- CCAT less sensitive than ALMA, but with full window bandwidth, CCAT can carry out spectroscopic surveys on galaxies with comparable speed.
- Can be even faster if coupling many galaxies at once.
- Future cryogenic space telescopes with background-limited spectrographs: ~1e-20 (but not funded!)

C+ Line luminosity fraction -> from Maiolano 05

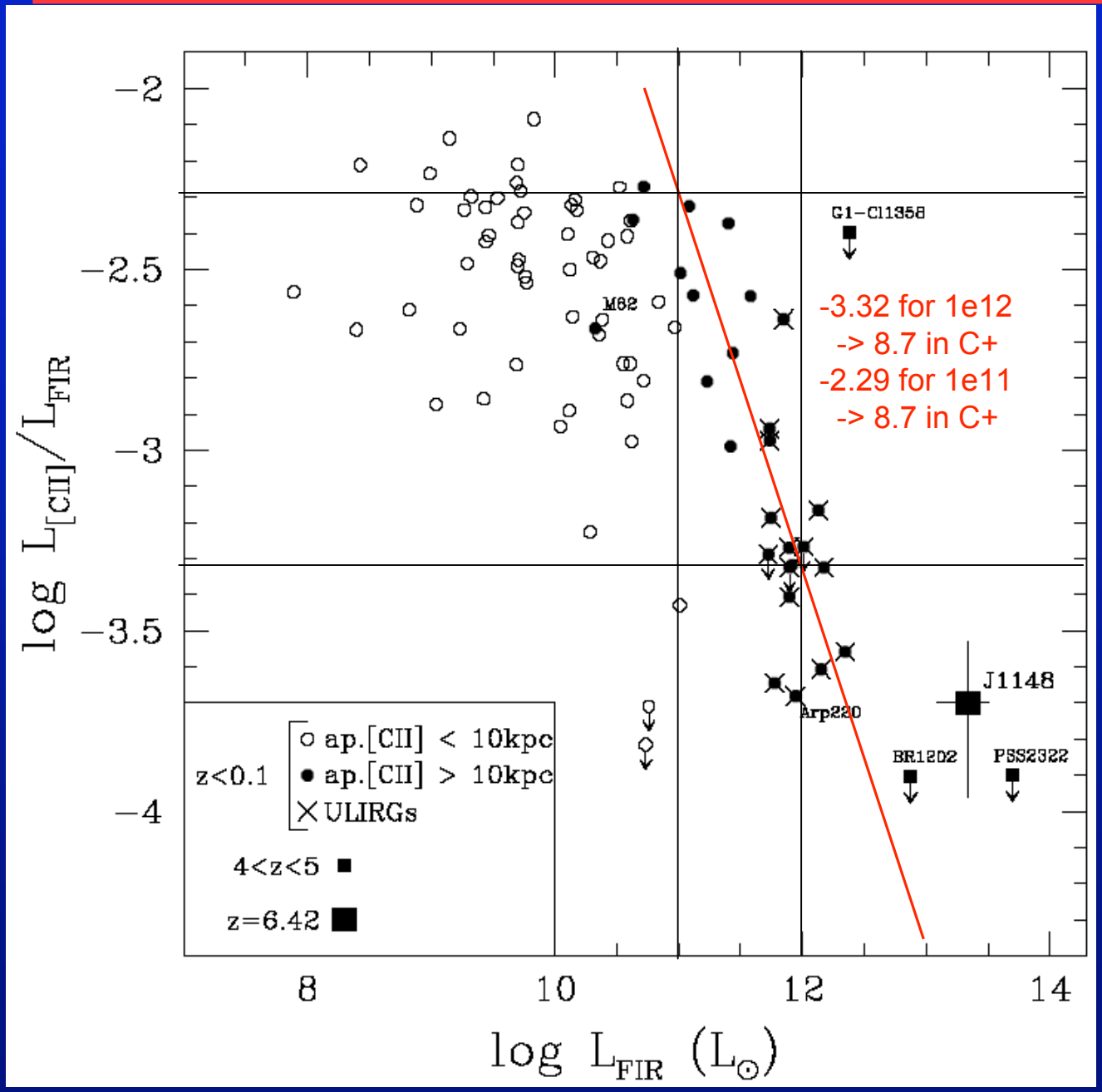

Local-universe LIRGS and ULIRGs have similar C+ intensities
-> Saturation of C+

Redshifted C+ Detectability with CCAT

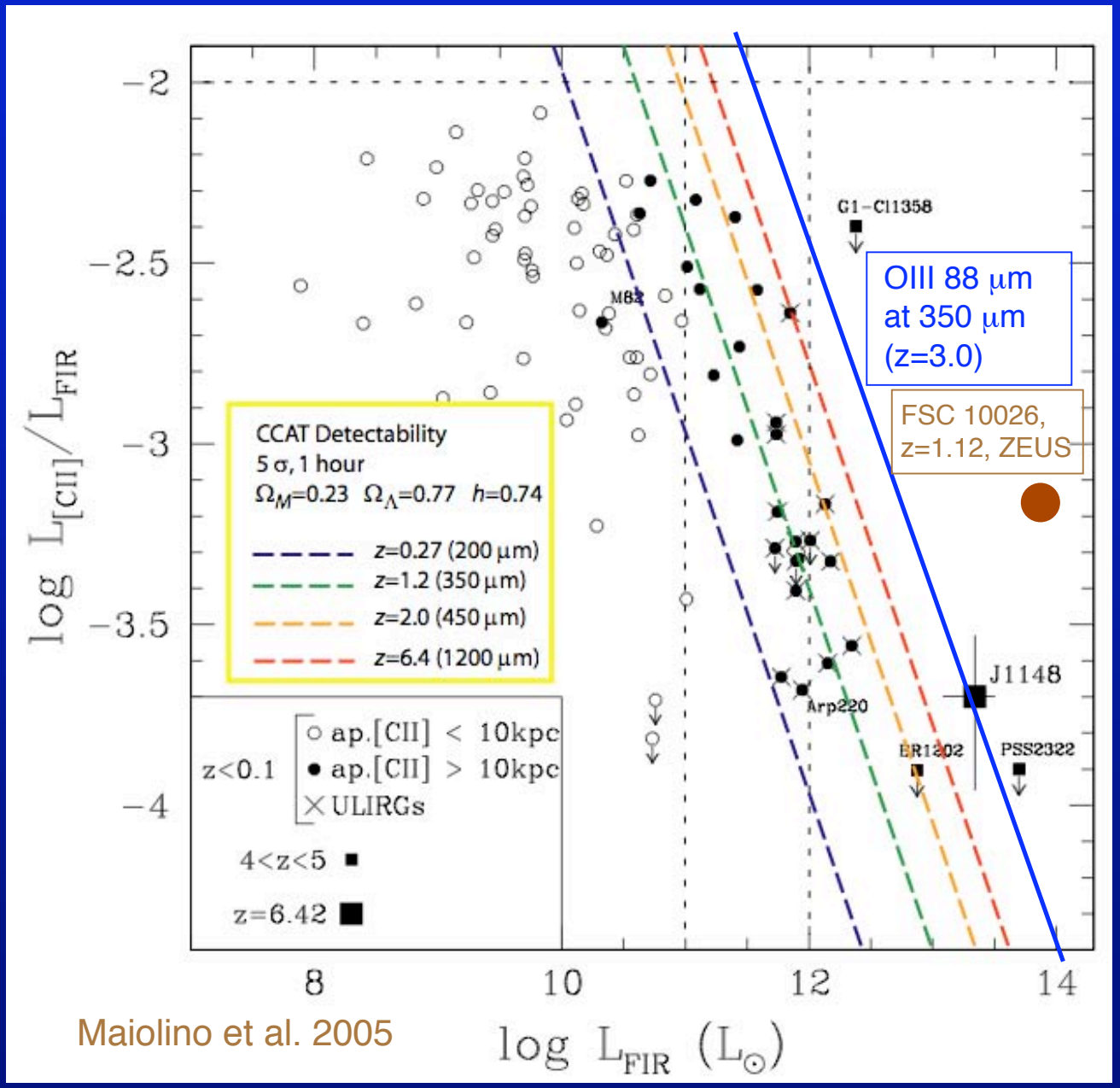

Maiolino et al. 2005

- *Constant C+ luminosity (log L_{C+}~8.7) for LIRGS to ULIRGS*

-> CCAT 350 μm sensitivities well-matched to these sources at redshift 1-1.4

- *88 μm [OIII] detectable for ULIRGS at z=3 if $f_{line} > 0.003$*

Source populations for CCAT C+ spectroscopy

MIPS 24 micron surveys:

biased toward low-z (z~1), but deep in L -- approaching knee at z~1 LIRG

Use SED model and photometric redshifts to derive luminosity function at various redshifts (Papovich, Perez-Gonzalez, LeFloc'h, Egami, et al.)

MIPS 24 reaches out to z~1 for LIRGS, z~2 with ULIRGS

Egami, LeFloc'h et al measure ~1440 galaxies per square degree with log L > 11.25 at 1.0 < z < 1.2

850 micron counts:

span the redshift range with almost uniform selection, but shallow in L

- ***shows redshift range, extrapolate to lower- L***

According to a reasonable 850 micron redshift distribution based on e.g. Chapman et al. measurements (w/ recent z~1 additions) or Benson model, the 1.0--1.2 redshift range should account for 5% of the total 850 micron sources at any given flux density.

This implies 3e4 total galaxies per sq deg with log L > 11.25 per sq deg ->

matched by 850 micron counts.

So we have a z~1 population measured at both 24 and 850.

MIPS 24um sensitivity, redshift selection

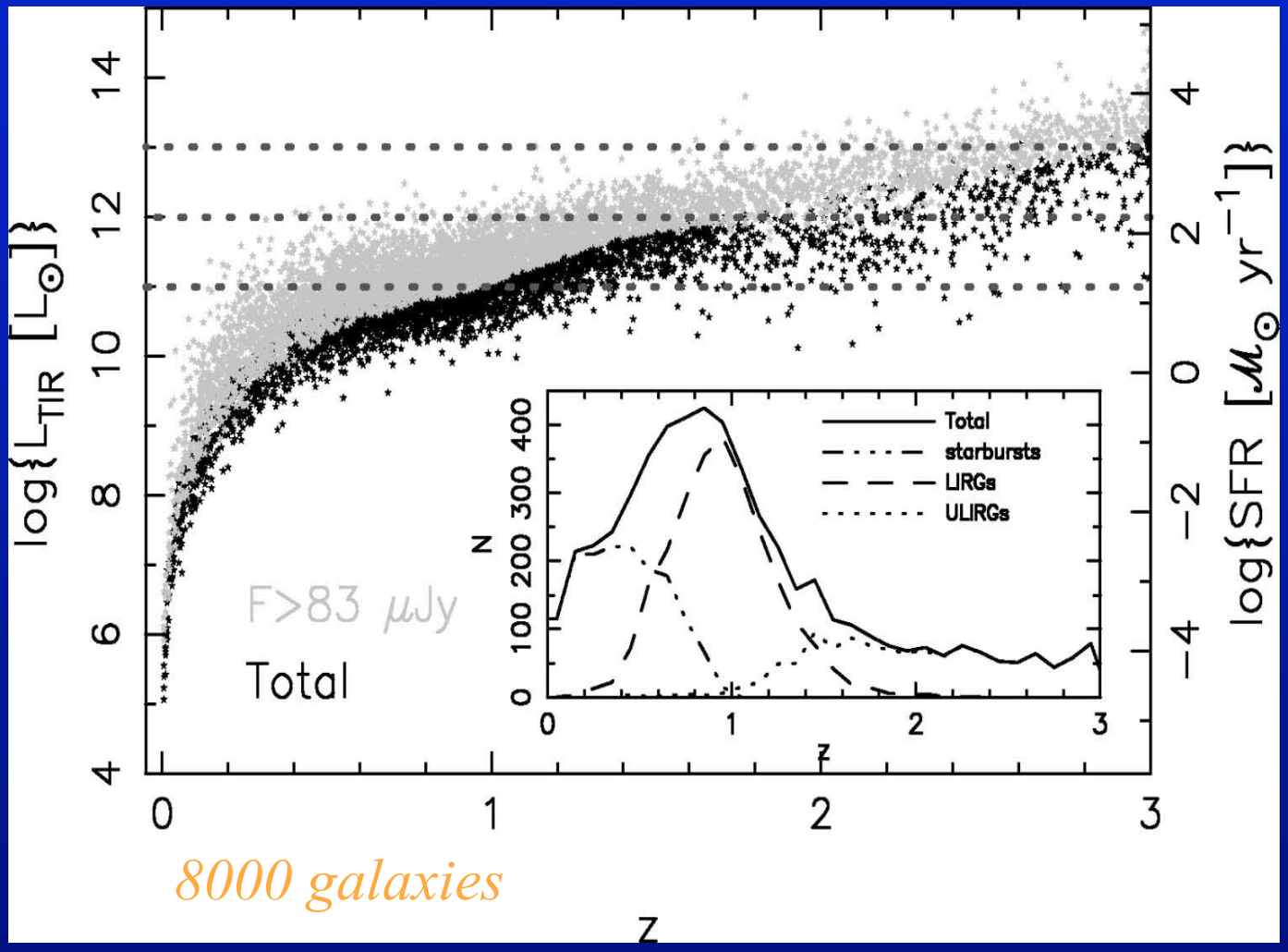

Perez-Gonzalez et al. (2006)

24 micron surveys (MIPS GTO team):

Spectroscopic and photometric redshifts

Use SED models to estimate luminosities from 24 micron fluxes

LIRGS to z~1, ULIRGS to z~2

850 micron N(S) is to first order a luminosity function

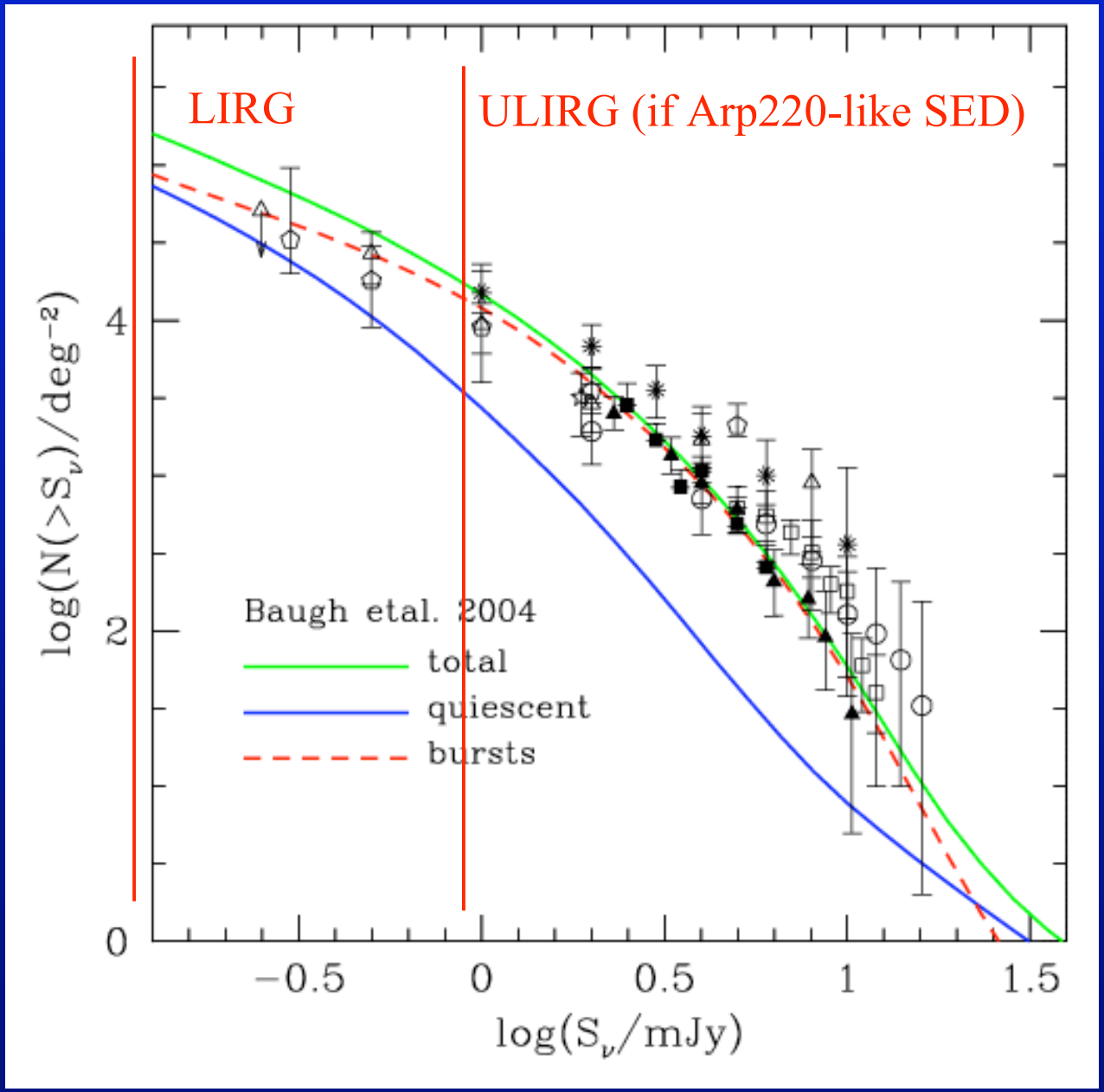

Models from A. Benson et al. (Galform group)

modified IMF and star formation timescale included to reproduce 850 micron counts

Models provide approach to CCAT population z distribution: Apply to C+

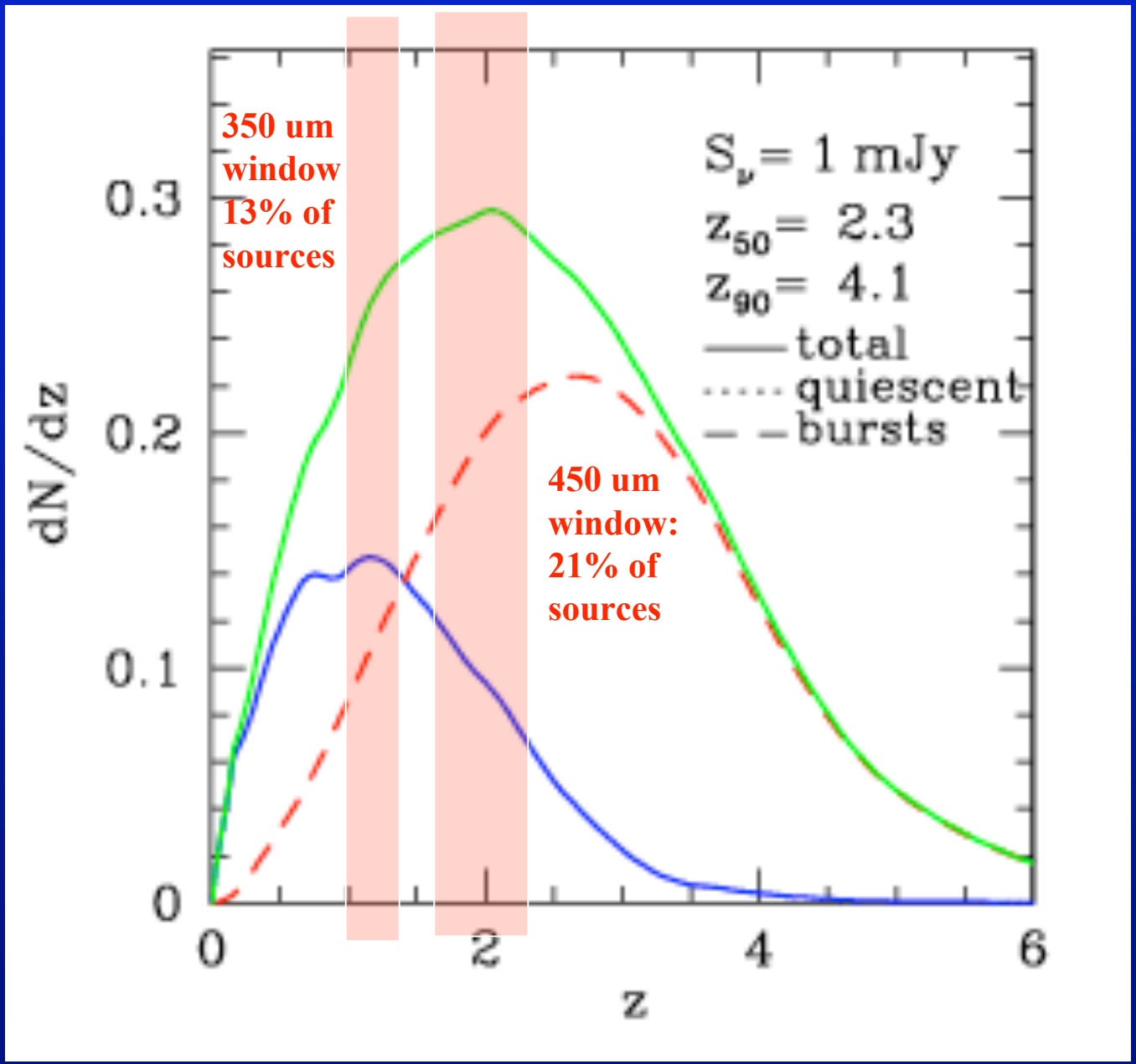

350 & 450 microns window are likely to access 31% of the 850 micron population in C+

Redshift Distribution from GALFORM model -- similar to Chapman

Source densities for C+ spectroscopy with CCAT

350 micron window

Redshift range 1-1.2 (low-z half of the window):

Density of Log L > 1e11 sources = 7.1 e4 x 0.2 x 0.24 = 3.4 e3

= **36 galaxies per square degree per 300 km/s spectral bin.**

= 1 source per 40,000 CCAT beams per spectral bin.

450 micron window (extrapolated)

Redshift range 1.8-2.0 (low-z half of the window) using a Chapman or Benson redhift distribution.

Density of Log L> 1e11 sources = 7.1e4 x 0.2 x 0.29 = 4.3 e3

= 62 galaxies per square degree per spectral bin

= 1 source per 14,000 CCAT beams per spectral bin

Options for CCAT spectrometers

- Grating spectrometer is the best choice for point sources.
  - 1st order → octave of instantaneous bandwidth
    - Potential for 350, 450 micron windows simultaneously
  - Good efficiency
  - Only moderate resolution
  - Potential for multi-object capability further multiplies efficiency
- Fabry-Perot naturally accommodates spectral mapping at discrete (known) frequencies.
  - Offers potential for high-resolution (R~10,000) over modest fields
  - But scanning time results in sensitivity penalty, esp for searching
- Fourier transform spectrometer (FTS) couples the full band to a single detector.
  - Sensitivity penalty
- Heterodyne receivers provide the highest spectral resolution.
  - But suffer from quantum noise

    $NEP_{QN} \sim h\nu\,[\delta\nu]^{1/2}$ vs. $NEP_{BG} \sim h\nu\,[n\,(n+1)\,\delta\nu]^{1/2}$
  - Also offer limited bandwidth:
    - 10 GHz IF bandwidth at 1 THz gives $\nu / \Delta\nu \sim 100$

C+ Detection Rate: Comparison Between F-P & Grating

Fabry-Perot

Source detection rate =

$dN / dz \times \Omega$

dN / dz = 36 -- 62 per square deg, per res el.

= 1.7e-2 sq deg

Rate = 0.6-0.7

Grating

Source detection rate =

$z\_fraction \times N\_mos$

z_fraction = 0.3 (including 350 & 450)

N_mos = ? (10-100)

Rate = 0.3 x 10-100

~FEW SOURCES PER HOUR

Could a Fabry-Perot serve to select sources at specific redshift from a field ?
Yes, but source densities are low enough that detection rate in the field will be low.
Broadband grating is faster if you can couple even a couple sources.

Most optimistic R=1000 FP at 350 microns: 200 x 200 = 4e4 beams or 1.7e-2 sq deg

Take 10 resolution element scan: Gives 1.7e-2 x 36 x 10 = 6 LIRG+ sources

In 10 hours observation. Doesn't look good, not enough volume due to finite z

NOTE ALMA: 3 times more sensitive -> 10 times faster per tuning
BUT MUST TUNE ~20 tunings to cover the full 350 / 450 bands

True broadband spectroscopy in the submillimeter: Z-Spec, a 1st order grating covering 190-305 GHz.

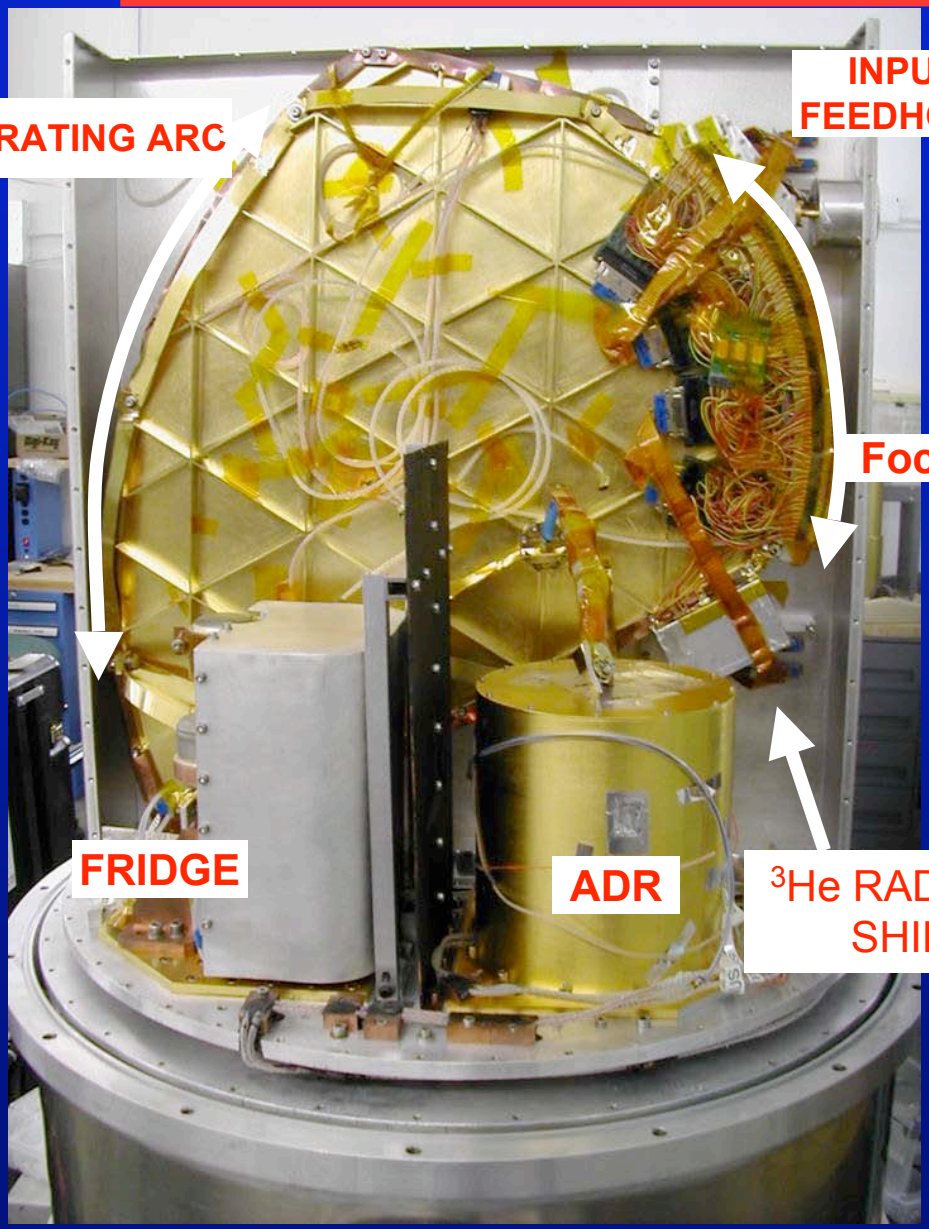

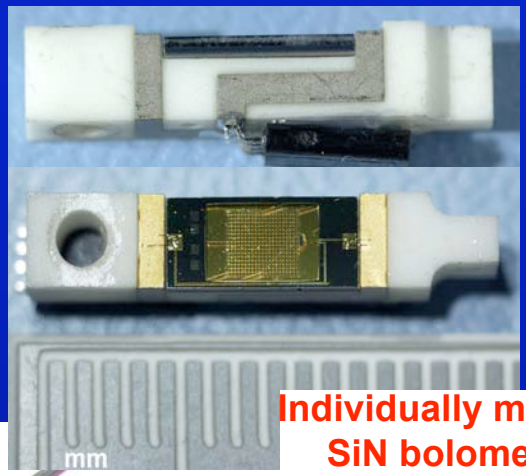

Individually mounted SiN bolometers

True Broadband Spectroscopy in the Submillimeter: Z-Spec, a 1st order grating covering 190-305 GHz

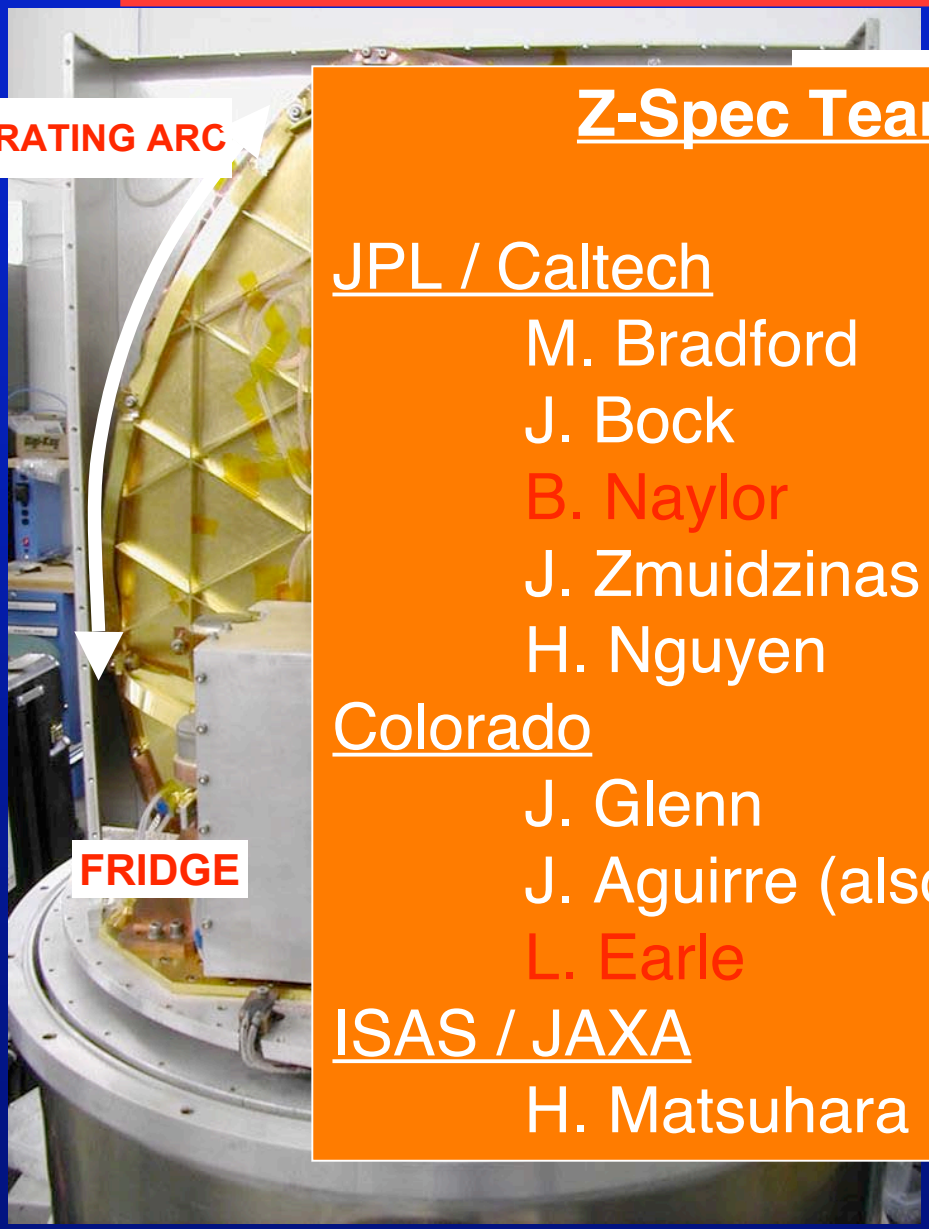

Z-Spec Team

JPL / Caltech
- M. Bradford
- J. Bock
- B. Naylor
- J. Zmuidzinas
- H. Nguyen

Colorado
- J. Glenn
- J. Aguirre (also NRAO)
- L. Earle

ISAS / JAXA
- H. Matsuhara

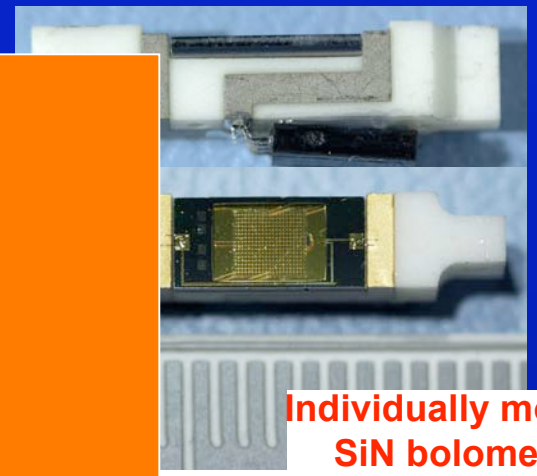

Z-Spec first results

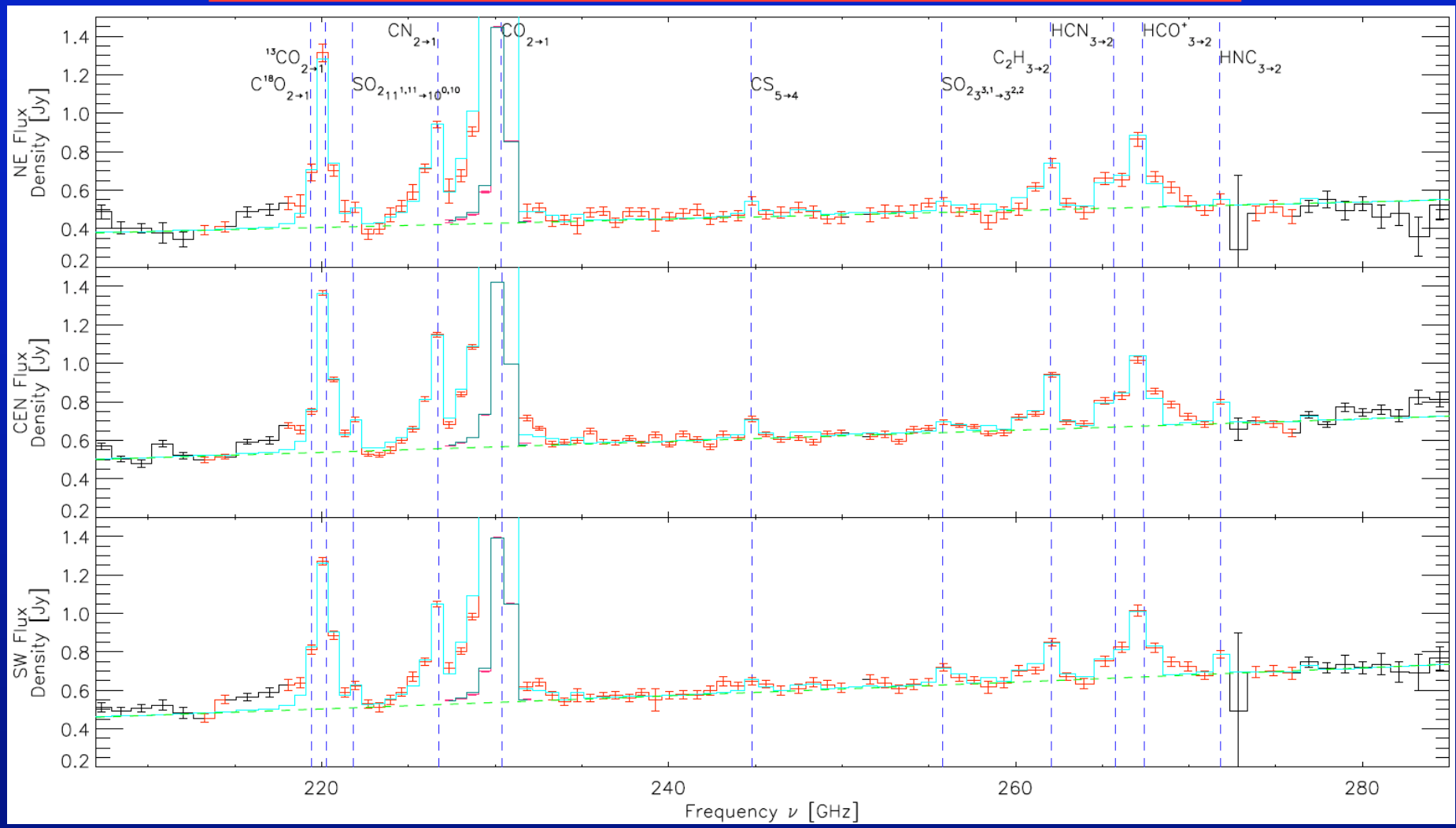

- At least 8 spectral features
- Excellent line-free continuum

Bret Naylor et al. (Caltech Ph.D. Dissertation, ApJ in prep.)

Z-Spec first results: Naylor et al., M82

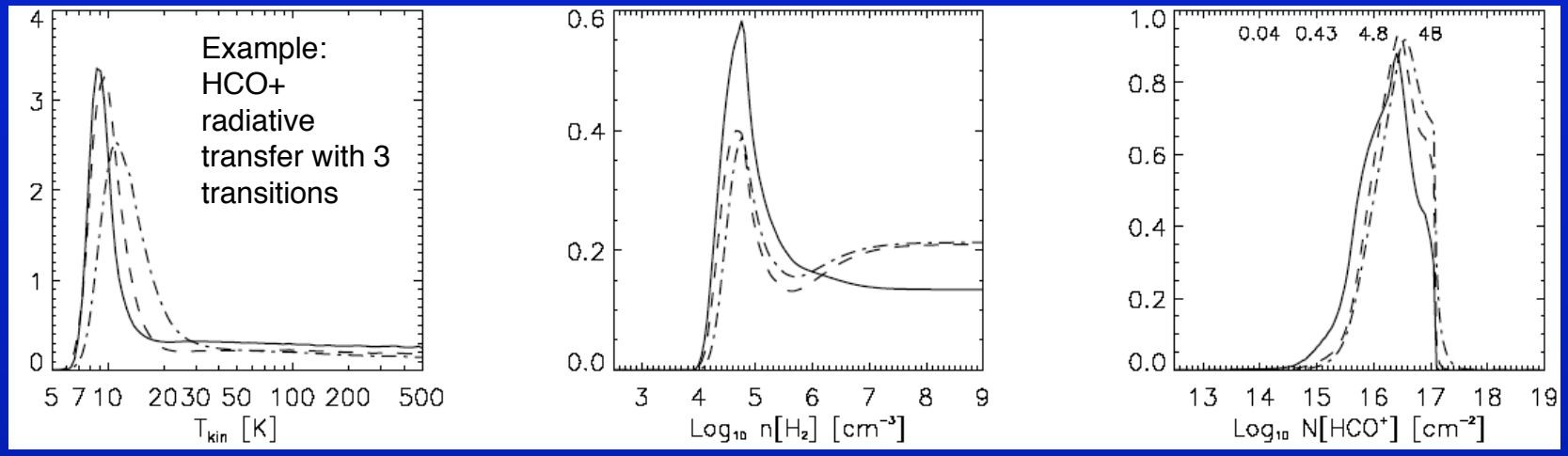

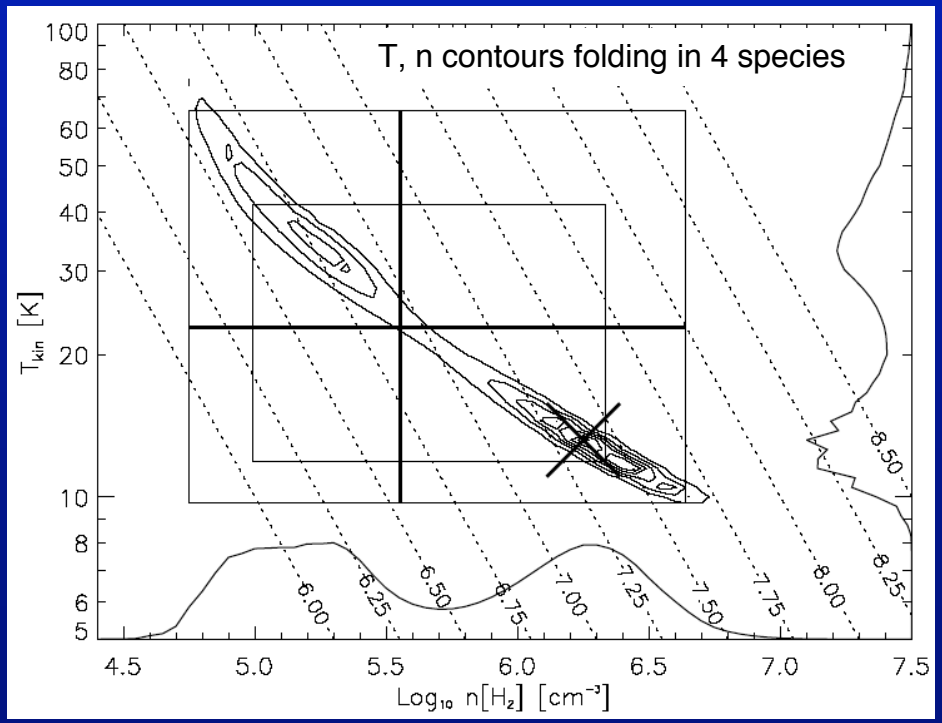

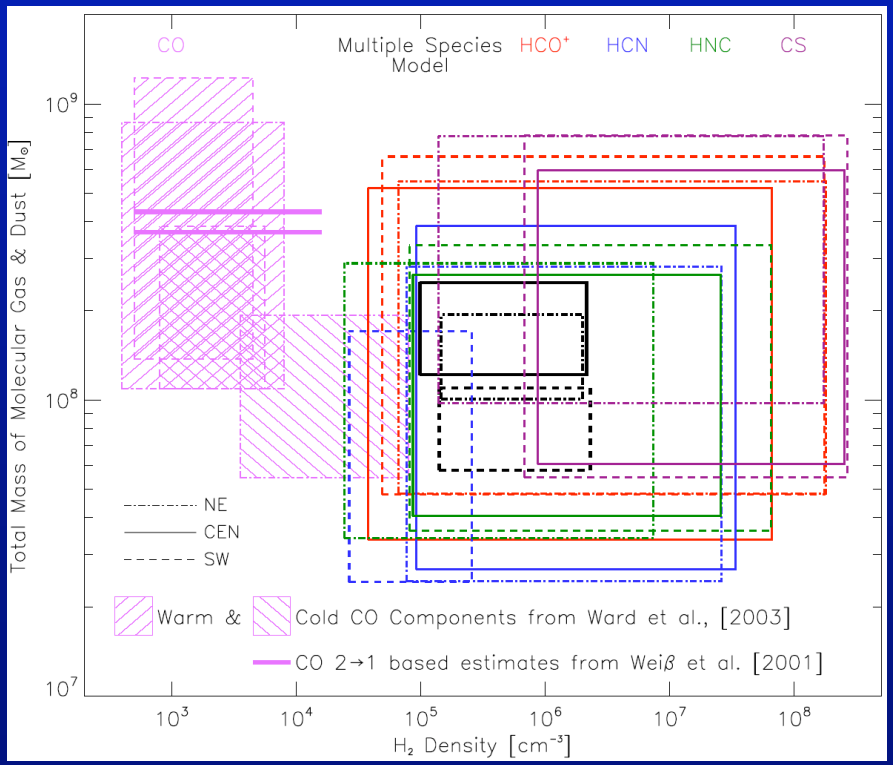

Z-Spec datasets at full functionality-- see also Lieko's talk

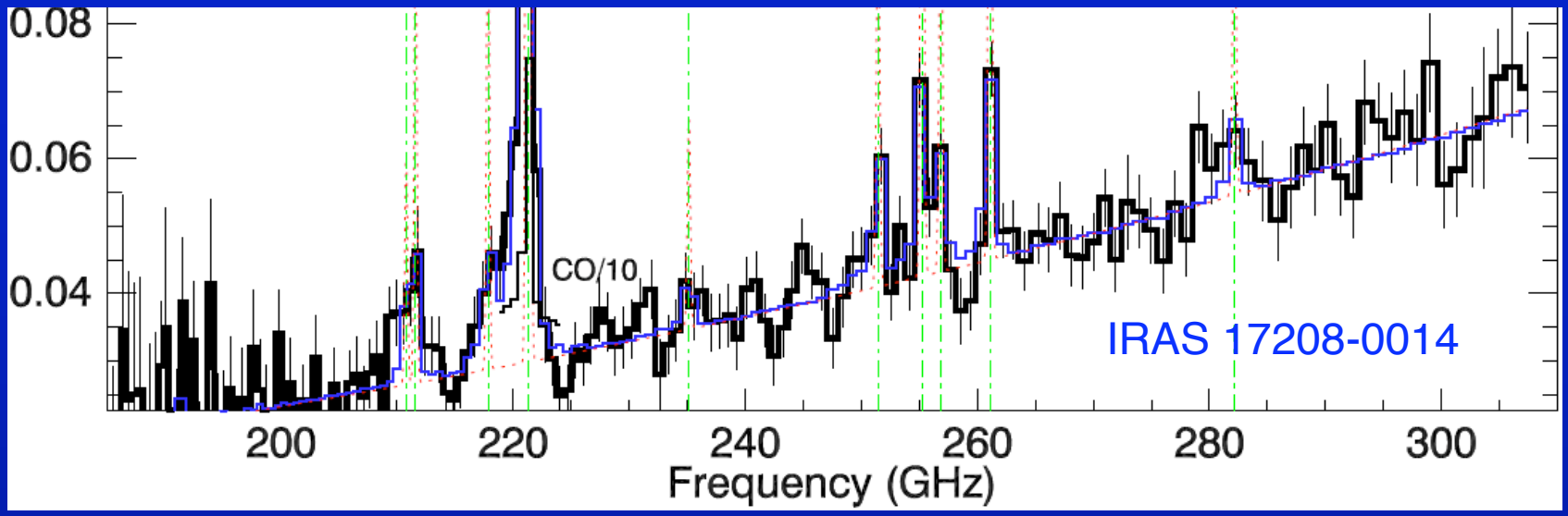

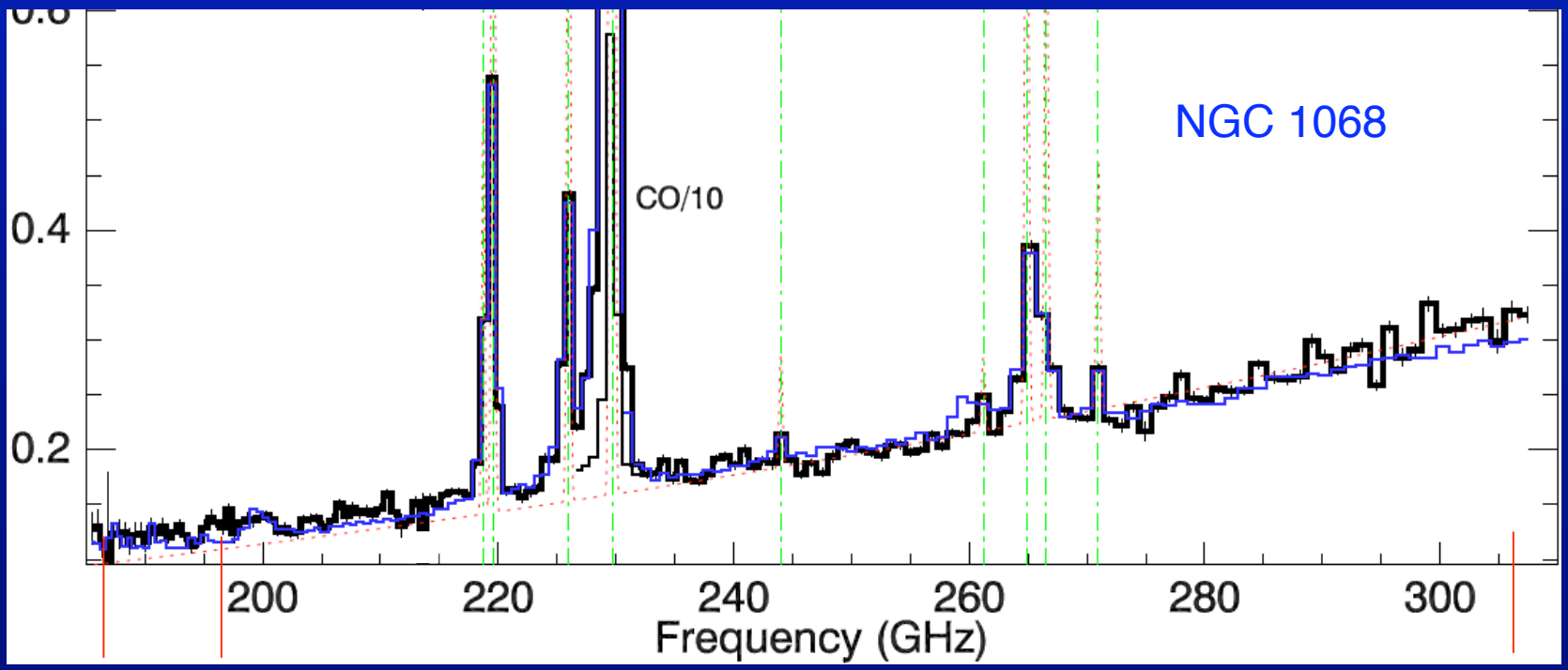

Z-Spec now beginning high-redshift compaigns

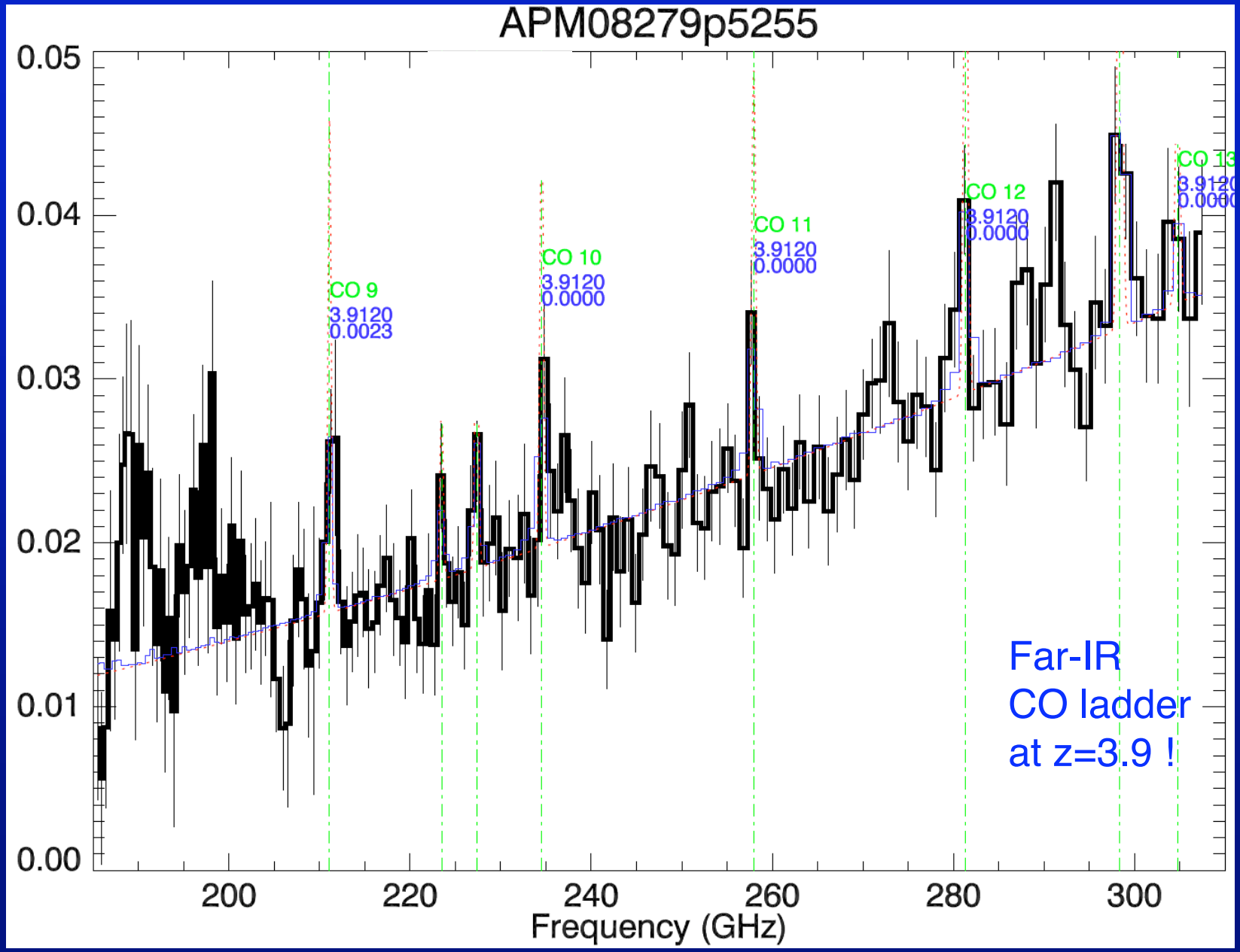

Both waveguide and free-space echelle grating spectrometers could accommodate a multi-object front end.

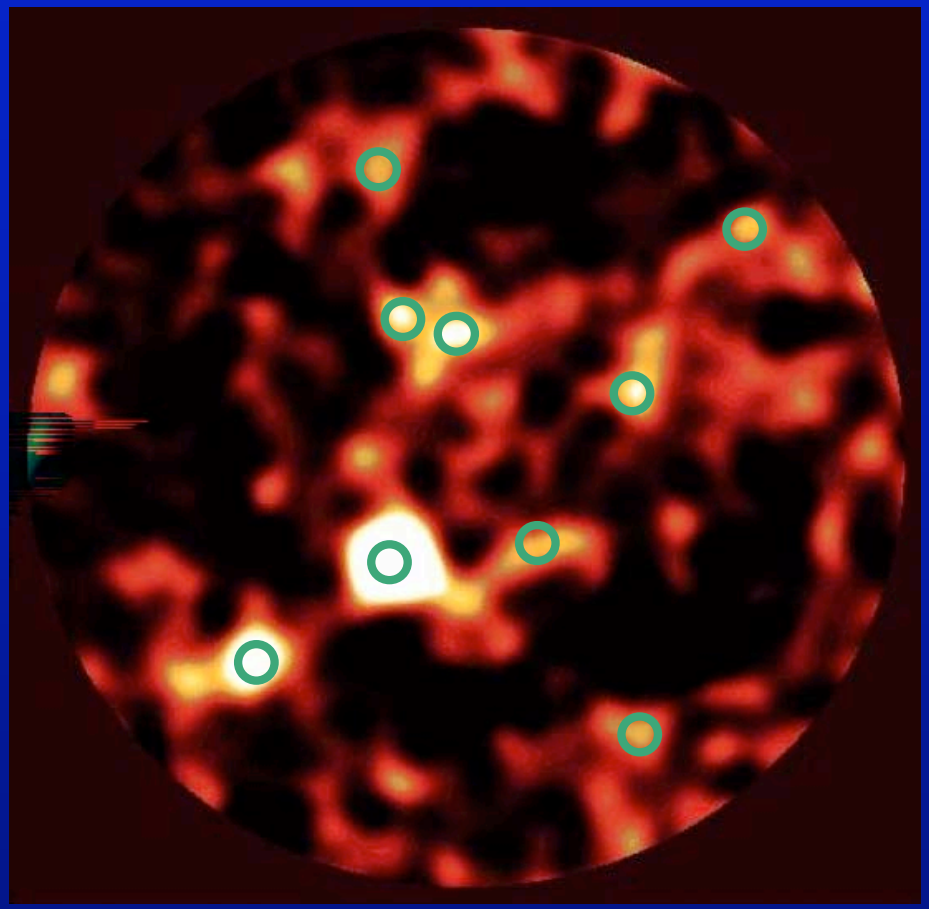

Hughes et al. SCUBA HDF North

- Remember CCAT continuum surveys at 350, 450 will go much deeper
- Will be ~110 LIRG+ galaxies in this 5.6 sq arcmin field.

Source density of LIRG+ galaxies:
71,000 per square degree
= 1 every 180 sq arcsec
= 1 every 10 CCAT 350 / 450 mm beams.

With slit of 1 x 30 beams:
Could position slit to get at least 2, perhaps 3 sources with no additional effort except field rotation.

Ideal system:

- 10-50 feeds patrolling 4 sq arcmin field.
- 8 x 8 cm in the native f/8 telescope focus.
- feeding slit of echelle or multiple Z-Spec-like devices
- Mirror arms or flexible waveguide

WaFIRS is an ideal broad-band point source architecture.
-- possibility for multi-object spectroscopy

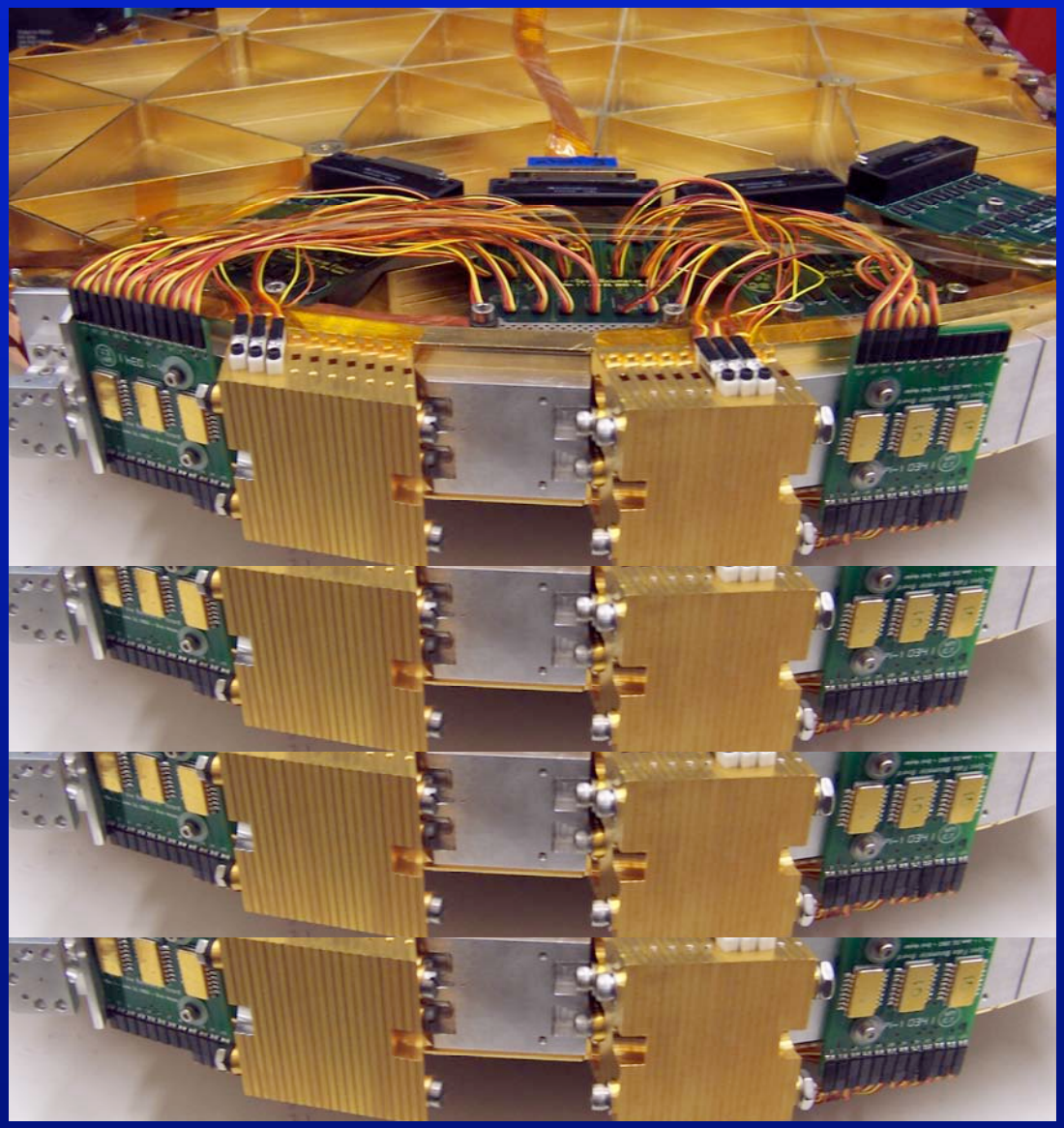

How many could be stacked ??

Currently 4-5 cm delta z per module, while propagation region is 2.5 mm

But could be smaller, far from limits:

-- stiffness of plates

-- detector illumination

-- feed (f lambda from the telescope)

Enabling a submm MOS: dielectric waveguide gratings

Z-Spec waveguide grating at CSO
R=300 for λ=1-1.6 mm -> 55 cm Al.

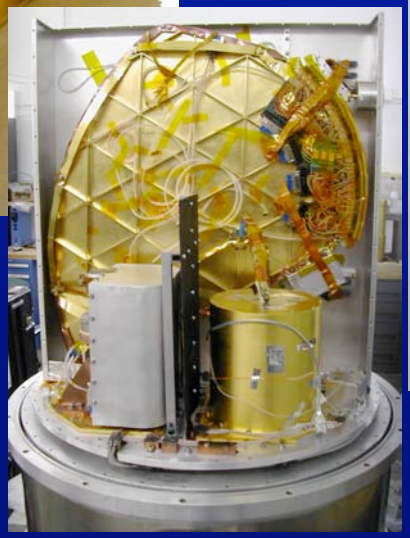

Large 60 mK cryostat required to get this grating cold!

Silicon-immersed waveguide spectrometer:
R=500 for λ=320-470 μm -> 10-cm wafer.

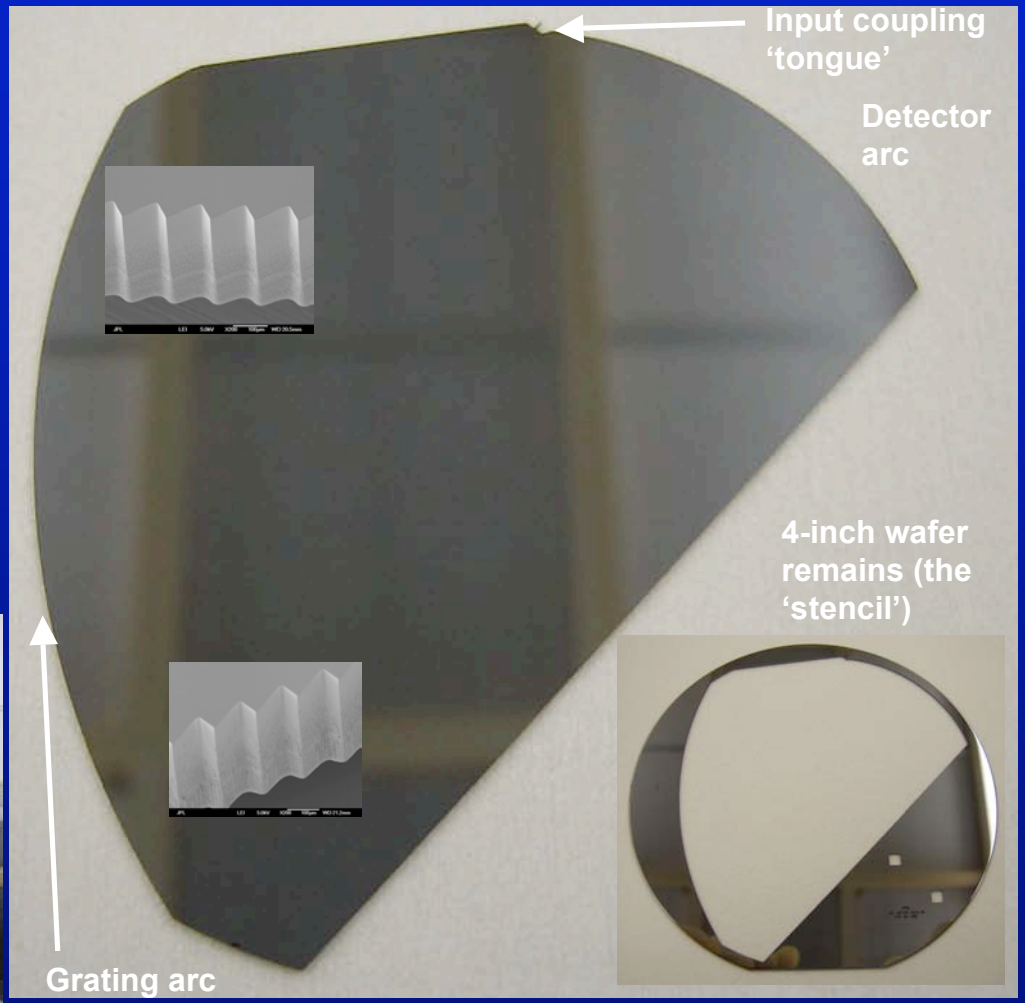

Etching courtesy Matt Dickie, Risaku Toda

Flexible low-loss submillimeter waveguide

need positioning in r~3 cm patch, < 20% loss in 20-30 cm propagation

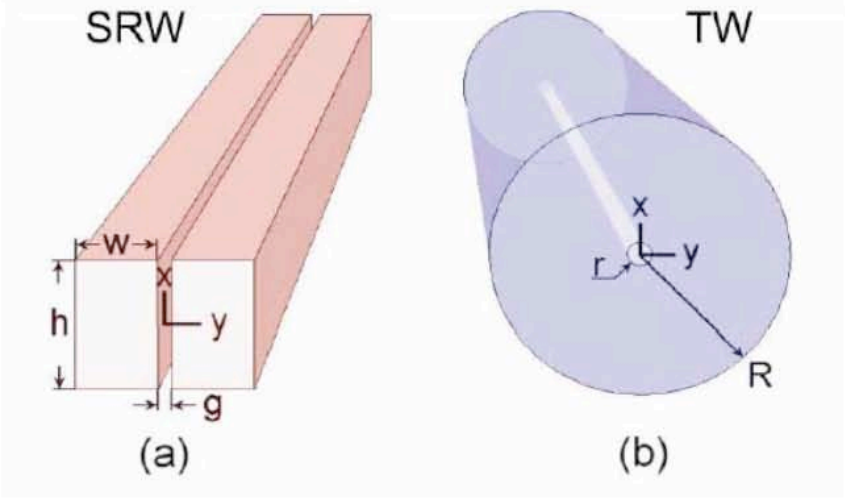

Fig. 1. Geometries of the considered dielectric waveguide structures: (a) A split rectangular waveguide and (b) a tube waveguide.

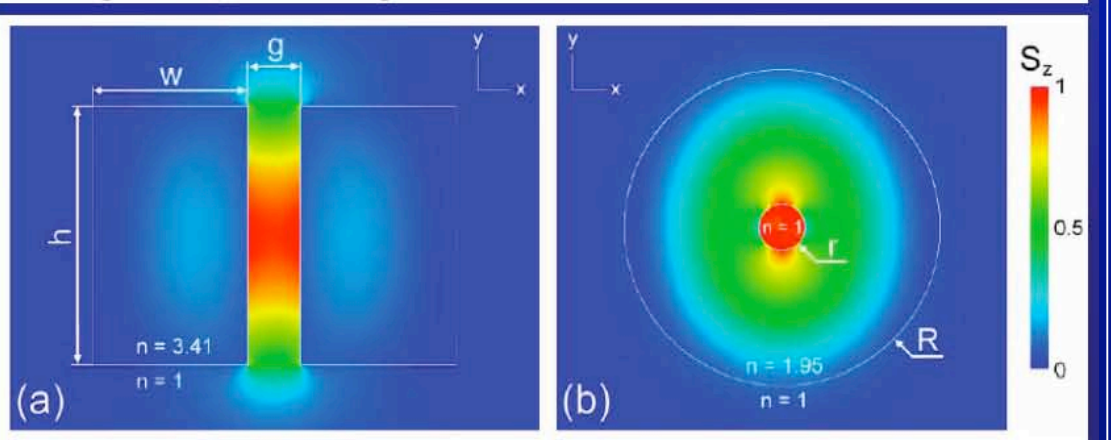

Fig. 2. Distribution of the normalized scalar z-component of the time-averaged Poynting vector S_z over a linear color scale in the cross section area of the waveguides. (a) Float-zone silicon split rectangular waveguide at $f = 0.7$ THz with $w = 54$ μm, $h = 90$ μm and $g = 18$ μm. (b) Fused silica tube waveguide at $f = 0.5$ THz with $R = 181.5$ μm and $r = 27$ μm.

Design will be a tradeoff between guiding to permit bends and reducing loss.

1) Dielectrics

But virtually all are lossy in the submm, --> try to concentrate the field energy in free-space

e.g. polyethylene monofilament, ribbon waveguide, SRW, TW

2) Free-space metal-walled guide

No dielectric loss, but ohmic loss -> choose mode to minimze this (generally this means overmoding, which can scatter upon bends)

e.g. VLA phase reference, Z-Spec spectrometer, Siegel et al silver-coated quartz tube.

Detectors for CCAT spectroscopy -- TES or MKID technology being developed for flight

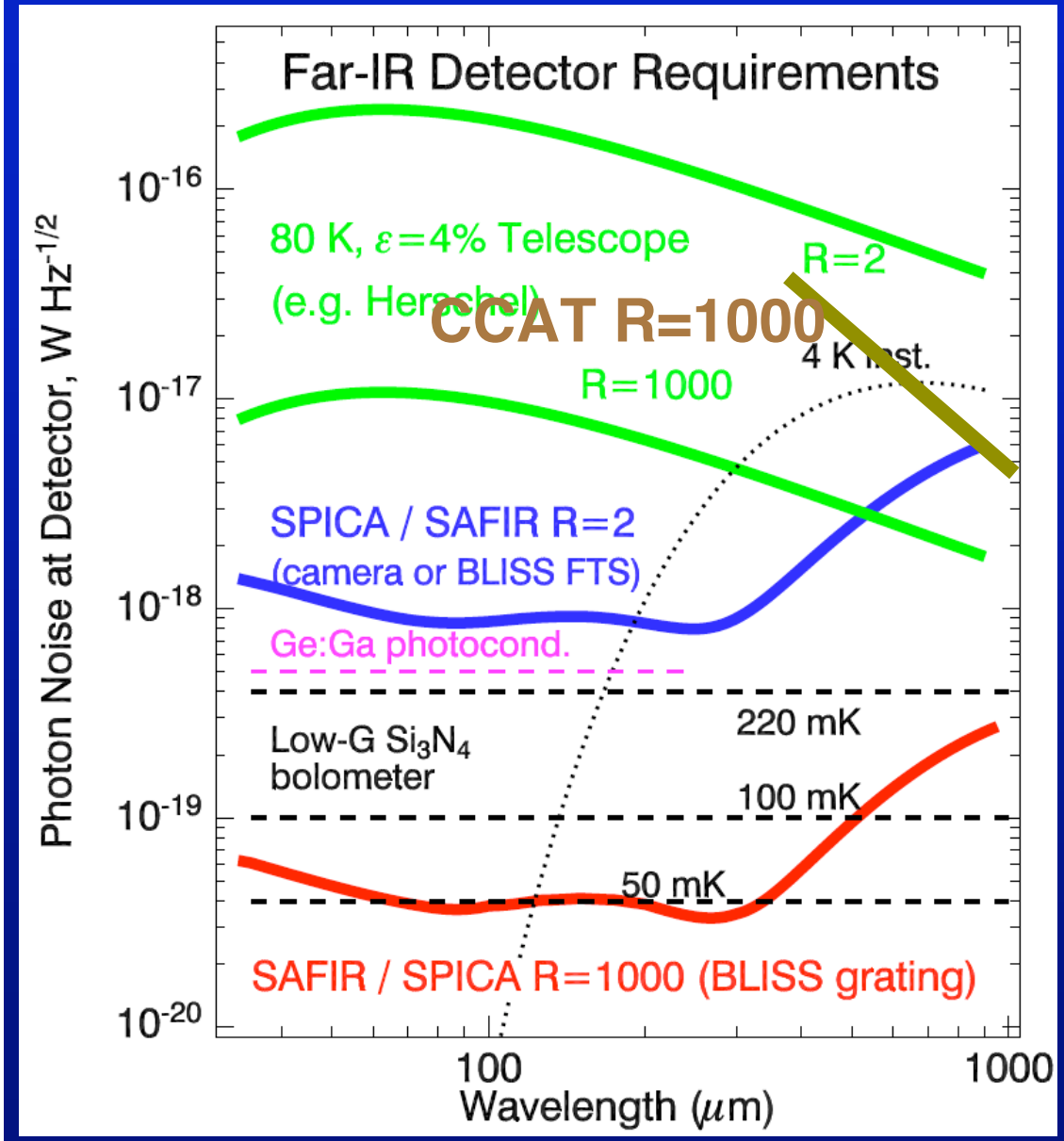

Want ~30 kpixel array for CCAT spectrometers.

Sensitive detectors are under development for low-background flight experiments.

Requirements for R=1000 at $\lambda <$ 1 mm with the CCAT are of order 10^{-17} W Hz$^{-1/2}$.

Achievable with existing devices.

TES MUX can work equally well at these NEPs -- development is similar to that of SW CAM, SCUBA-2.

R~10,000 at the long wavelengths starts to become a relevant testbed for SAFIR / SPICA detectors.

4 K instrument: $A\Omega$ = 3 mm^2, $\Delta\lambda/\lambda$ = 50 %, ε = 10 %

Conclusions

- Tens of thousands to millions of galaxies will be discovered in far-IR to millimeter continuum surveys in the next 15 years.
- Spectroscopic follow-up will be the bottleneck.
- CCAT can be competitive with ALMA for spectral surveying in the short submillimeter.
  - a multi-object broadband grating can exceed ALMA for spectral-survey follow-up of LIRG+ galaxies.
- Galaxies w/ $L > 10^{11}$ have ~constant C+ flux and are detectable with CCAT spectrograph.
  - ~1 hour in the 350 micron band
  - ~4 hours in the 450 micron band
  - together these bands will capture ~30% of all the 850 μm-selected sources
- Existing spectrographs with modest upgrades can reach close to the fundamental photon-noise limits of CCAT.
- Ideal CCAT spectrometer is a multi-object low-order grating. Technology for this is under development.
  - We CAN get redshifts: few to couple tens per hour.

extras

MIPS 24um; IR Luminosity Evolution

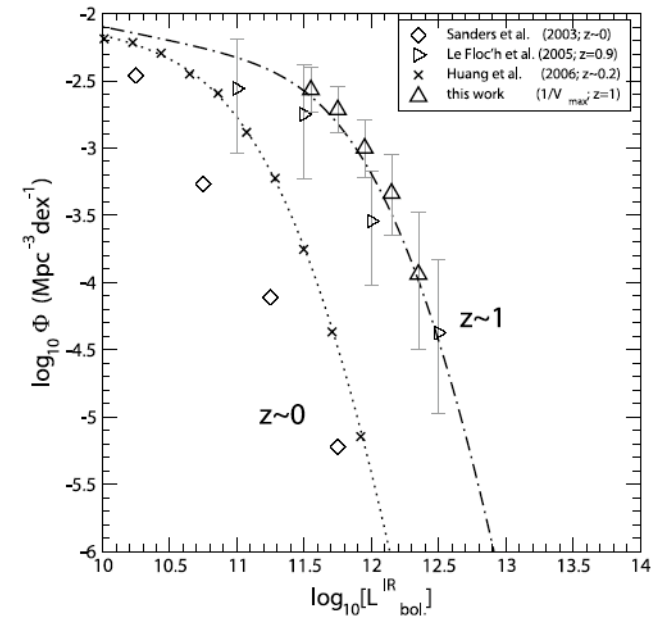

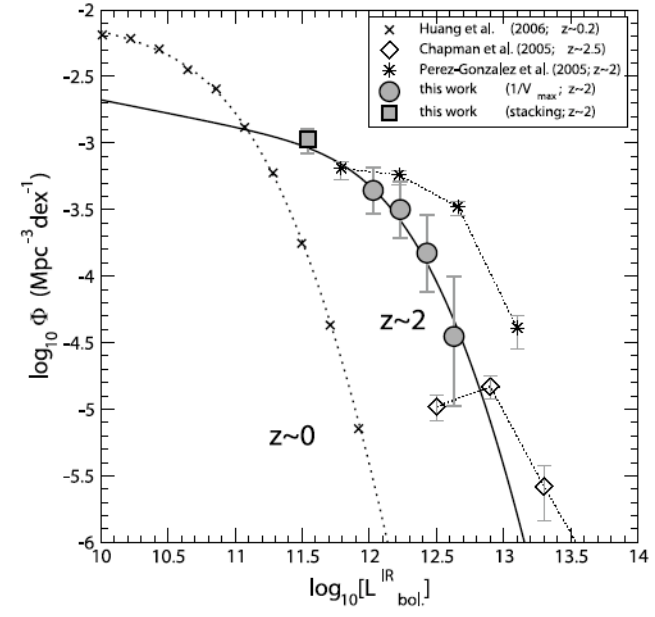

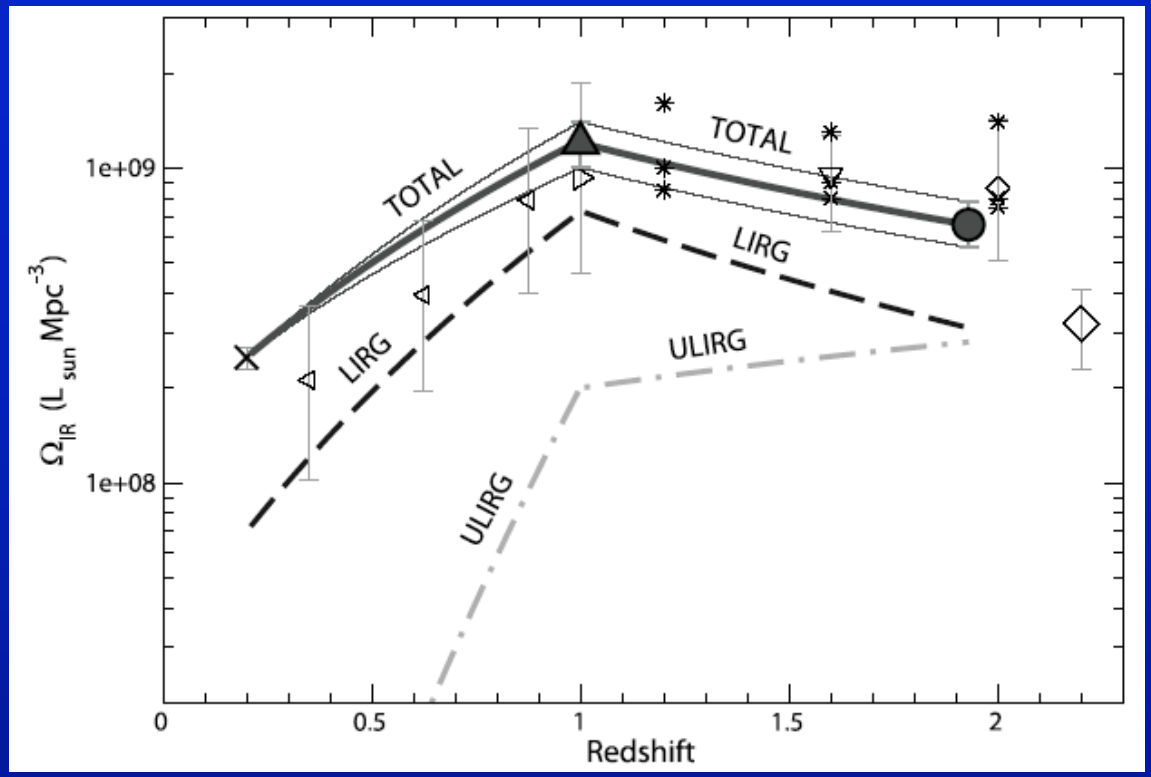

8-micron luminosity functions converted to total IR luminosity functions
-> comoving luminosity density

MIPS team Caputi et al. 2007, ApJ 660:97-116

Z-Spec labor force

Bret Naylor
Caltech Ph.D. student
(finishing August)

James Aguirre
Jansky Fellow
Colorado, NRAO

Lieko Earle
Colorado Ph.D. student
(finishing Dec)

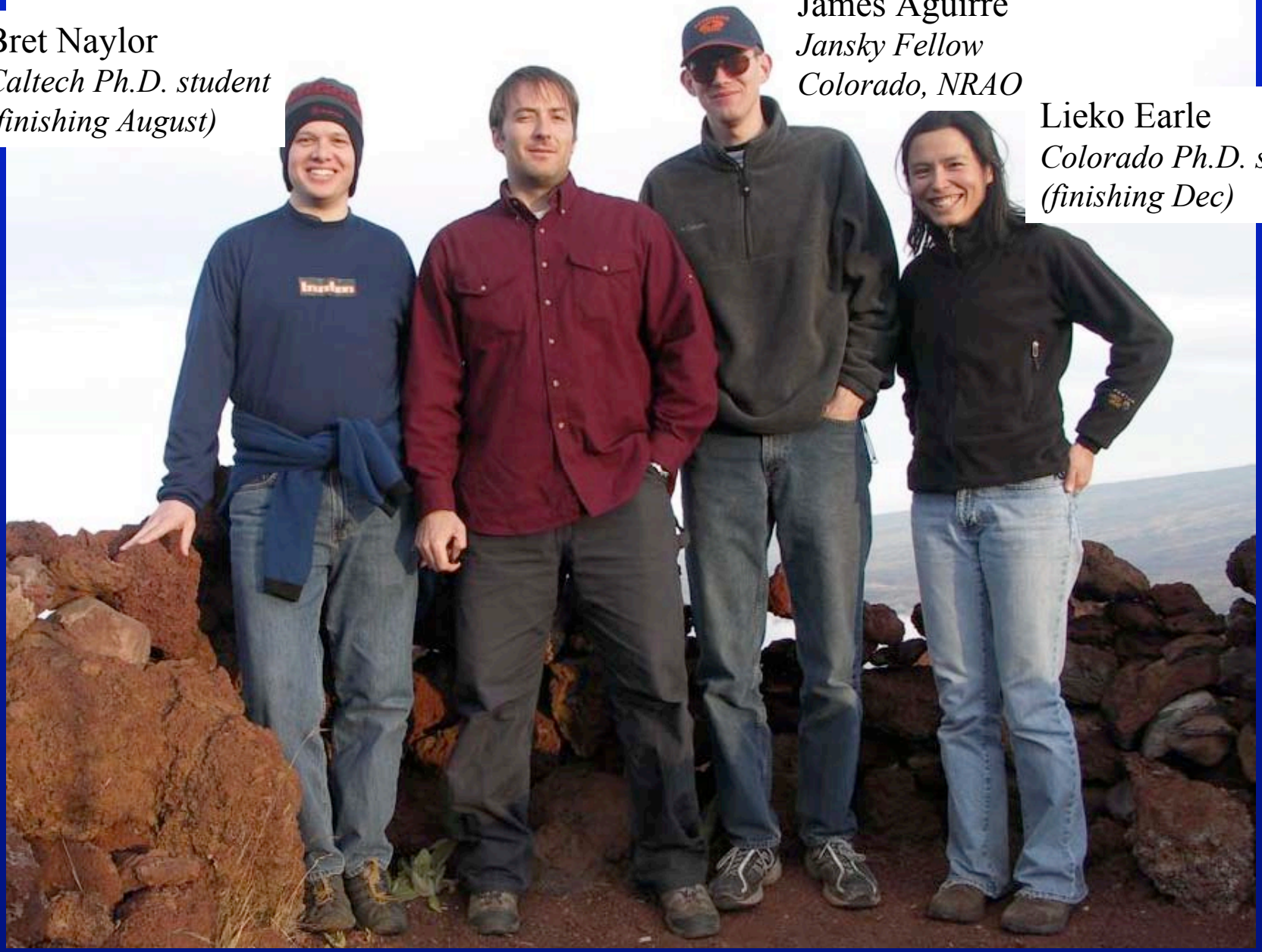

Examples of submillimeter-wave echelle grating: ZEUS for the JCMT / APEX

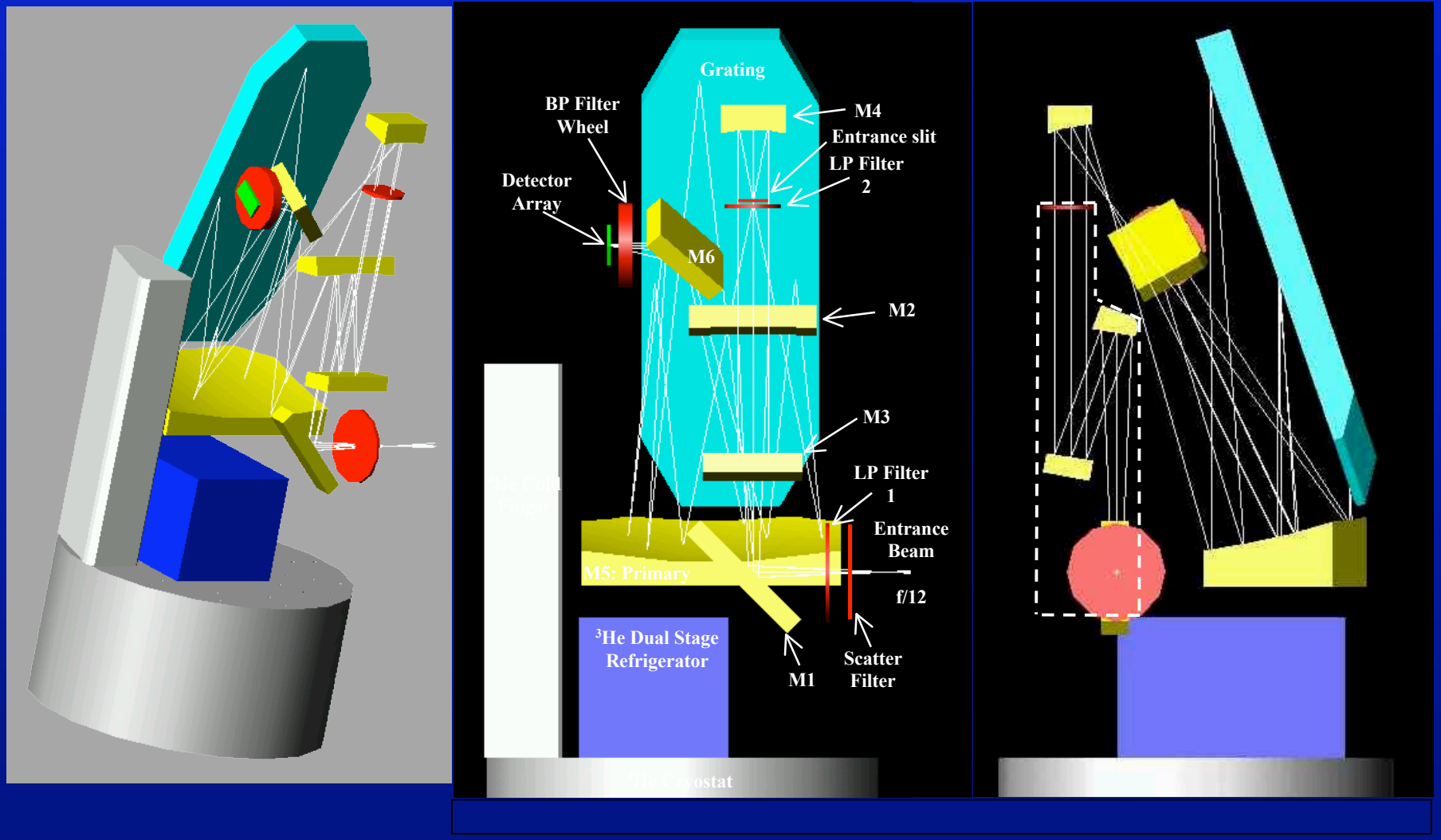

Cornell -- Stacey, Haley-Dunsheath, Nikola

350, 450 μm windows w/ R~1000-1500

ZEUS Grating

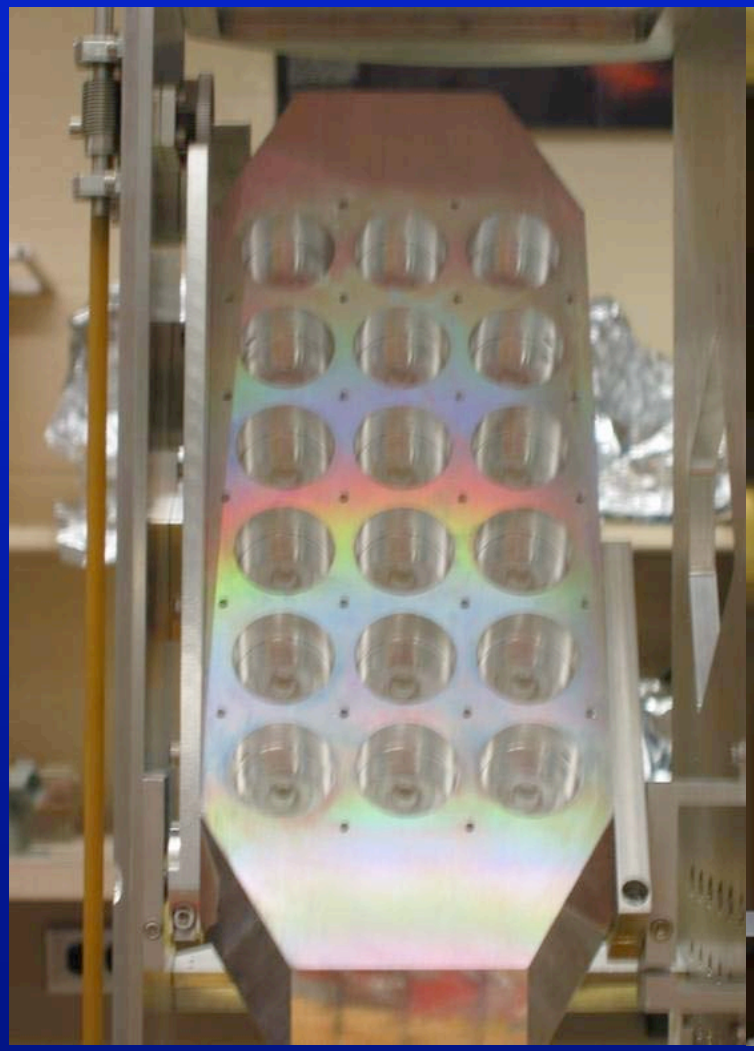

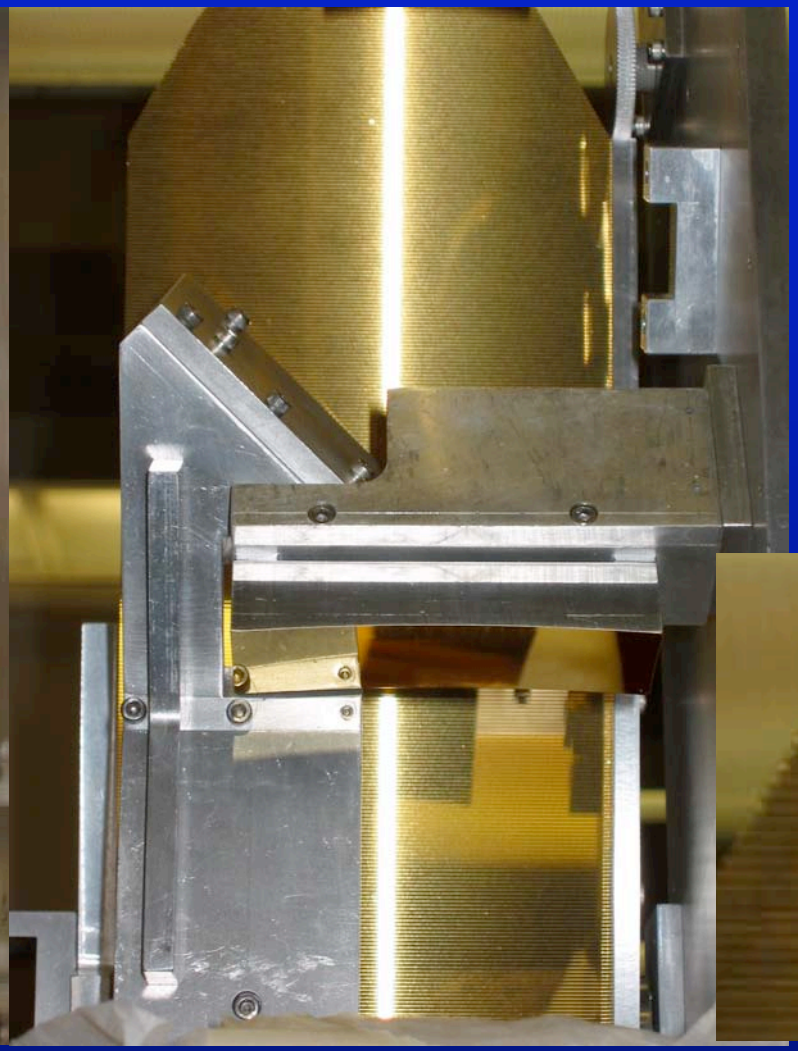

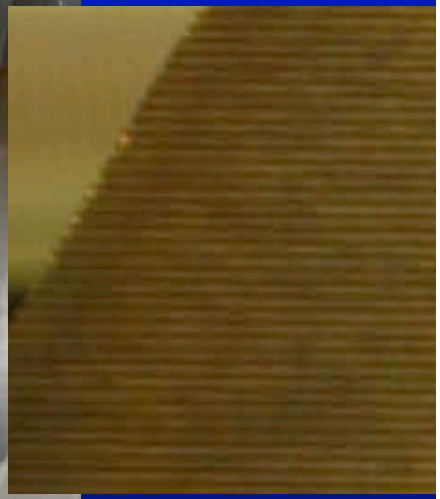

- *Manufactured by Zumtobel Staff GmbH (Austria).*

ZEUS on the CSO

First Run: March 2006

Steve Hailey-Dunsheath

Gordon Stacey

Flexible waveguide feeds:
polyethylene monofilament?

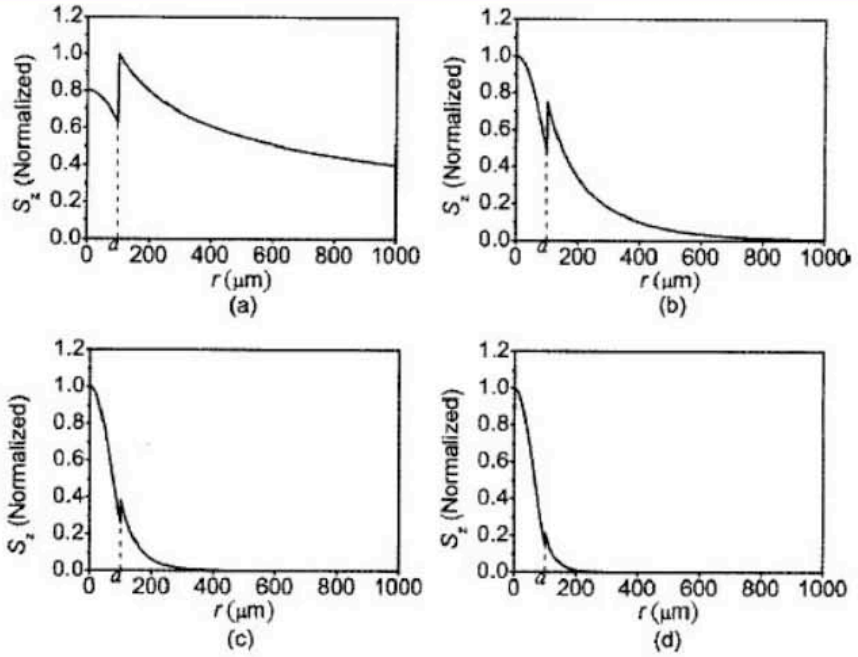

Fig. 1. Spatial distribution of the z-direction Poynting vector about a 200 μm diameter ($a = 100$ μm) PE wire at frequencies of (a) 300, (b) 500, (c) 700, and (d) 900 GHz. The PE wire is assumed to be surrounded with air.

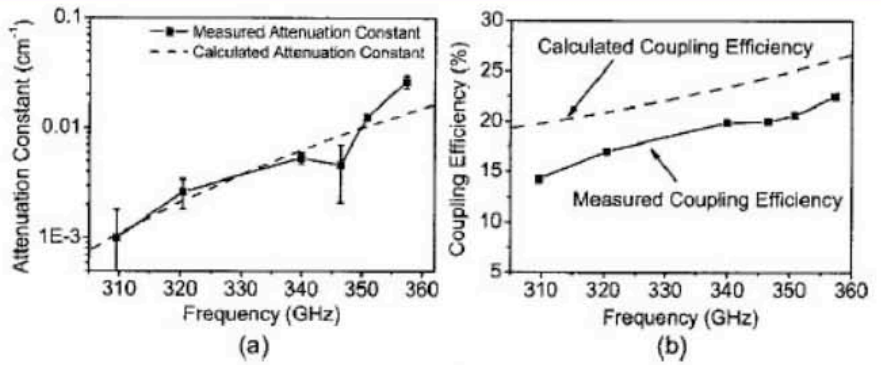

Fig. 2. (a) Measured fiber attenuation constant of the 200 μm diameter PE wire in the frequency range 310–360 GHz. For comparison, the calculated fiber attenuation constant of an ideal THz fiber, whose absorption constant α is assumed to be 1 cm^{-1} in this frequency range, is shown. (b) Comparison of measured and calculated coupling efficiency of the PE wire in the frequency range 310–360 GHz.

Chen et al. 2006

$$\alpha_f = \left| \frac{1}{P}\frac{dP}{dz} \right| = \frac{\sigma \int |E|^2 d\tau}{\left| \int S_z d\tau \right|},$$

Tradeoff between guiding and loss
less field inside -- lower loss but
cannot bend sharply.
NEED BENDING MEASUREMENTS

CCAT echelle will be large

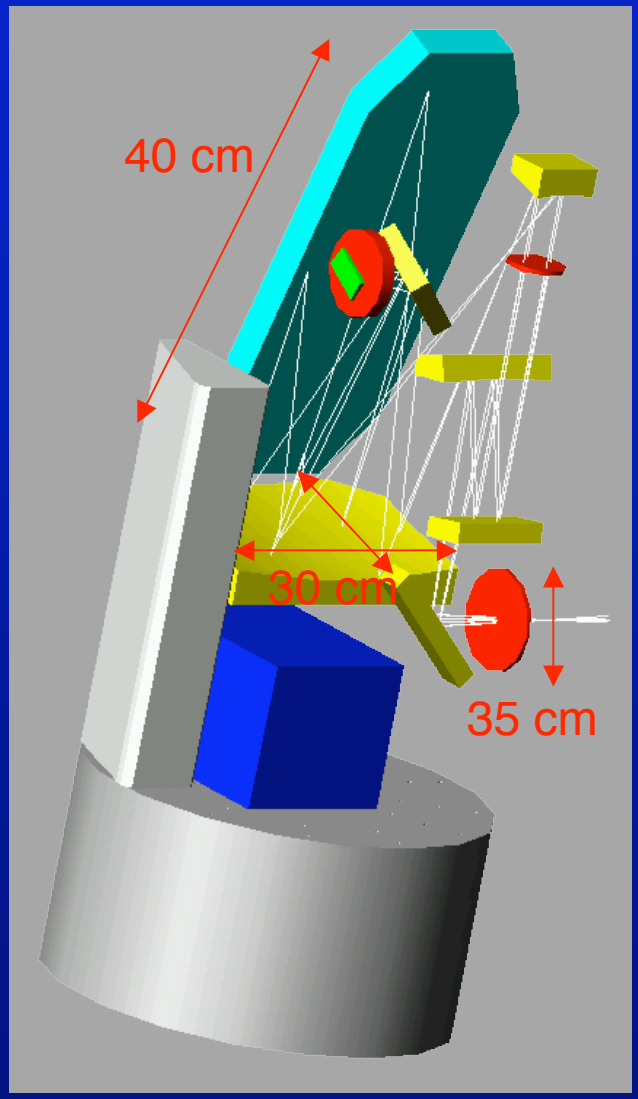

So grating and collimator are a large fraction of 1 meter in all dimensions -- 1.5-2 times larger than ZEUS

Reimaging optics size will depend on the size of the slit, but also grows relative to ZEUS:
--scales as telescope f# x #of beams: Relative to ZEUS, CCAT echelle will have 8/12 x 128/32 = 2.7 times larger reimaging optics.

- **Requires 35 cm (+ overhead) window if reimaged from telescope focus inside cryostat (but can be shaped like a slit)**

Optics envelope inside cryostat approaching 1 meter in all dimensions.

Large but doable.

Redshifted C+ Detectability with CCAT

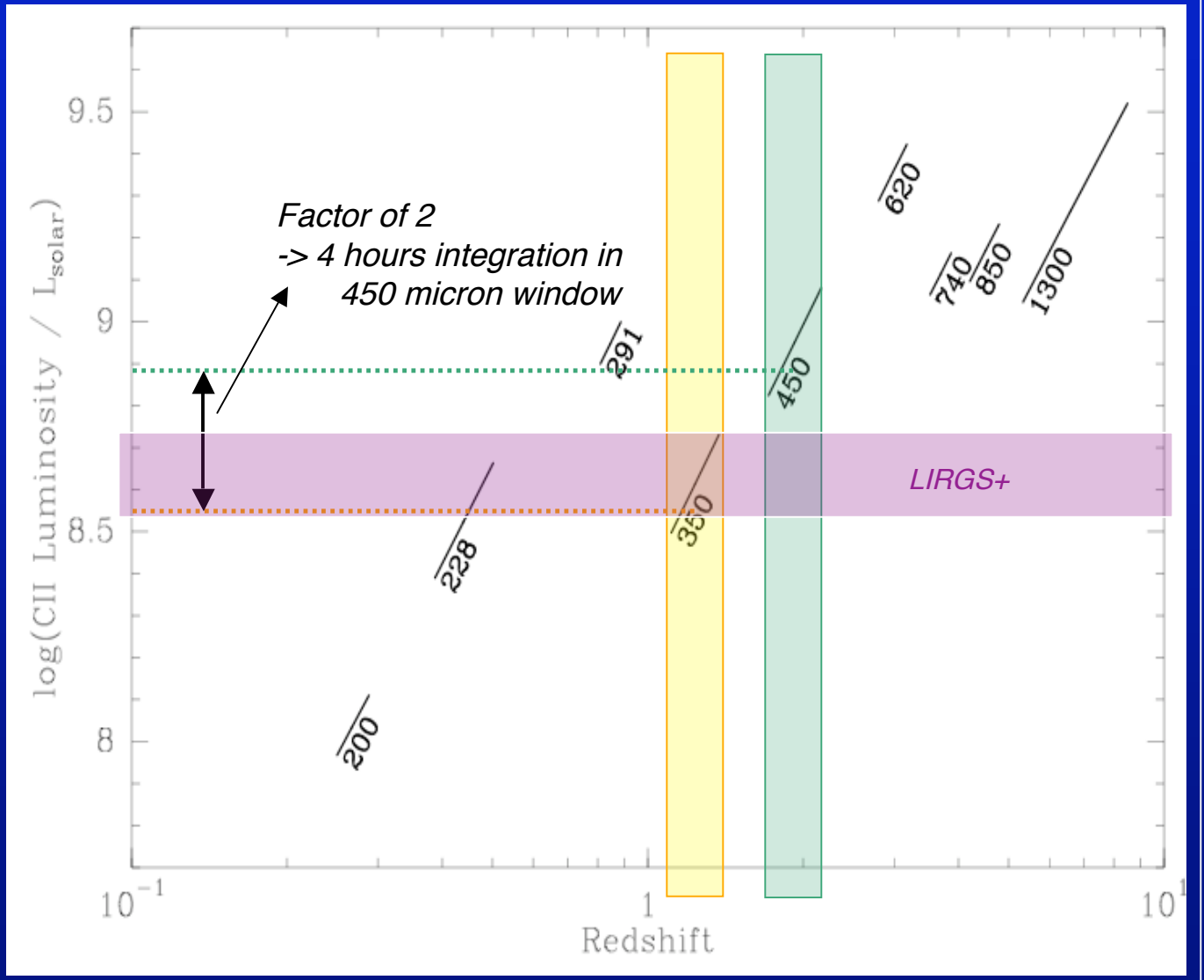

- Constant C+ luminosity (log L_{C+} ~ 8.7) for LIRGS+

-> CCAT 350 μm 1-hour sensitivity well-matched to these sources at redshift 1-1.4

- 4 hours @ 450 μm (z ~ 1.8-2.2) for the same sources.

How many such sources are there per area per redshift?

The Physics of the [CII] Line

The [CII] to far-IR continuum luminosity ratio, R is a sensitive indicator of the strength of the ambient ISRF, G

- In high UV fields (young starbursts, ULIRGS, AGNs), R is depressed
  - Reduced efficiency of photoelectric effect
  - Increased cooling in [OI] 63 μm line
- More diffuse fields (like M82 and the Milky Way) result in ***larger*** [CII]/far-IR ratio

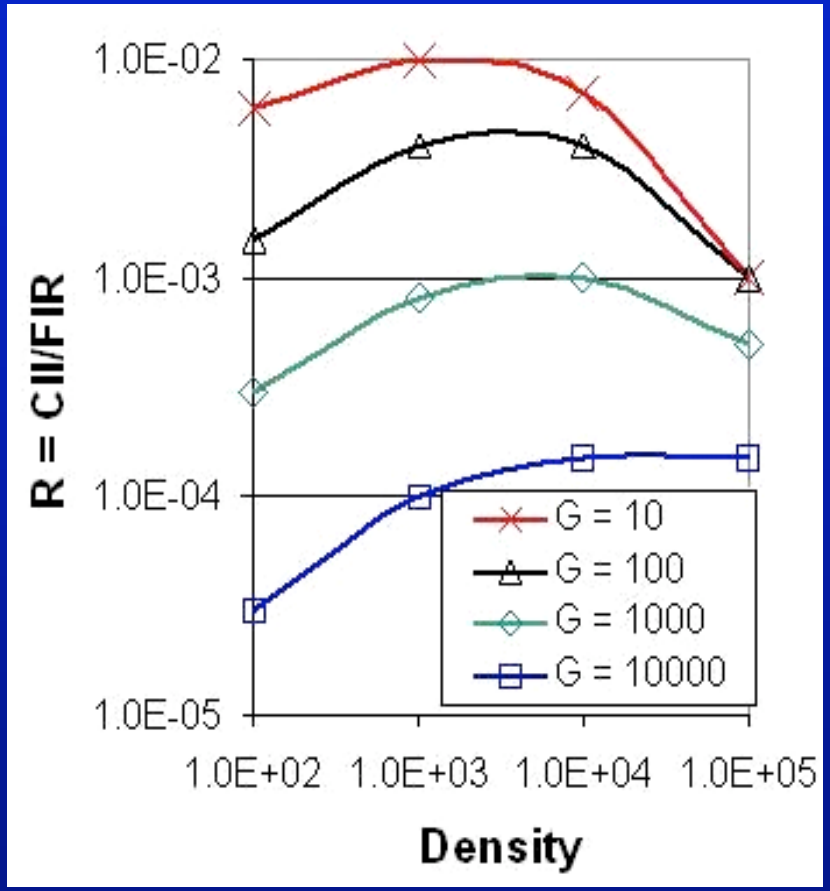

Fig. 2 [CII]/far-IR continuum luminosity ratio vs. density for various G (from Kaufman et al.).

Gordon Stacey

The Physics of Redshifted [CII]

- For sources with unit beam filling factor, G and $I_{far\text{-}IR}$ are equal
- Therefore the ratio of the observed quantity, $I_{far\text{-}IR}$, to the derived quantity, G, is equal to the source beam filling factor, or ***physical extent of the starburst.***
- ***Notice that it is extremely useful that we can detect the underlying continuum simultaneously with the line – a strong advantage for using a broadband direct-detection system.***

Are starbursts extremely localized (and vigorous) in SMGs, or are they extended?

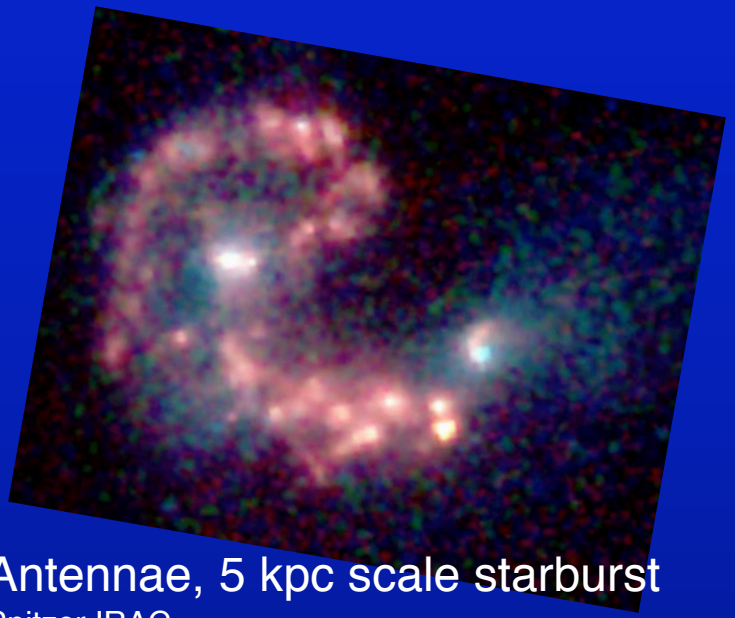

Antennae, 5 kpc scale starburst
Spitzer IRAC

Arp220, Activity concentrated in central kpc. ISO CAM

C+ in an IRAS Galaxy at z = 1.12

25”

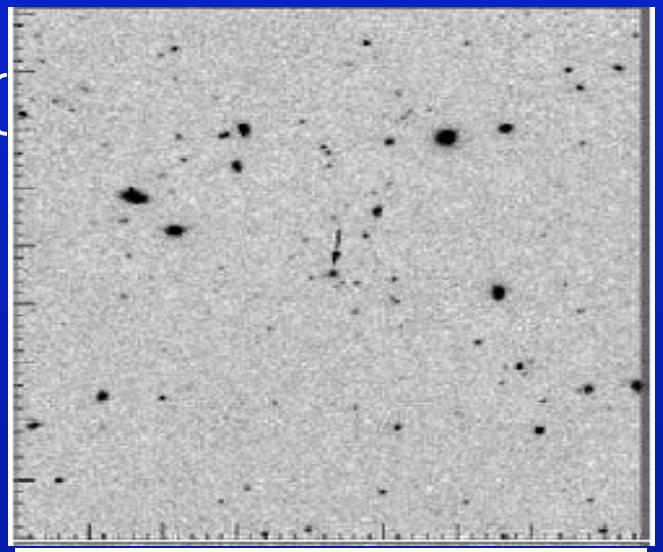

K_s band image of FSC10026+4949 (Farrah et al. 2004)

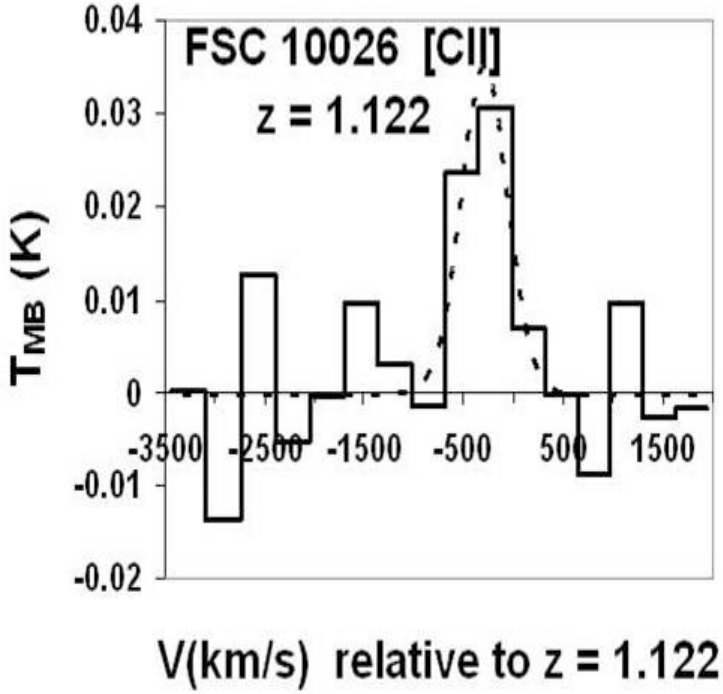

ZEUS/CSO (Hailey-Dunsheath et al. 2007)

- Detected [CII] line (S/N = 6.4) FSC10026+4949 using ZEUS on the CSO (t_{int} ~ 1 hour, $t_{l.o.s.}$ ~ 20%)
- $L_{far\text{-}IR} \sim 6.5\times10^{13}\ L_\odot$ (Duncan et al. 2004) and $L_{[CII]} \sim 4.5 \times 10^{10}\ L_\odot$
  $\Rightarrow R \sim 7\times10^{-4}$

Gordon Stacey

Bright C+ at high-z: Implications

- $R \sim 7 \times 10^{-4} \Rightarrow G \sim 2000$
- Beam ~ 11”
  - $\Rightarrow \chi_{Far\text{-}IR} \sim 55$
  - $\Rightarrow \phi \sim \chi/2 \div G \sim 1.4\%$
  - $\Rightarrow d_{source} \sim 10$ kpc

Starformation is extended on kpc scales

- Agreement with Chapman (2004) et al. results:
  - unlike local ULIRGs, starformation in 8/12 SMGs is galaxy-wide
  - Scales ~ 45 kpc^2
  - Rates ~ 45 $M_\odot/yr/kpc^2$
- Far-UV radiation field high, but not unlike local starbursters

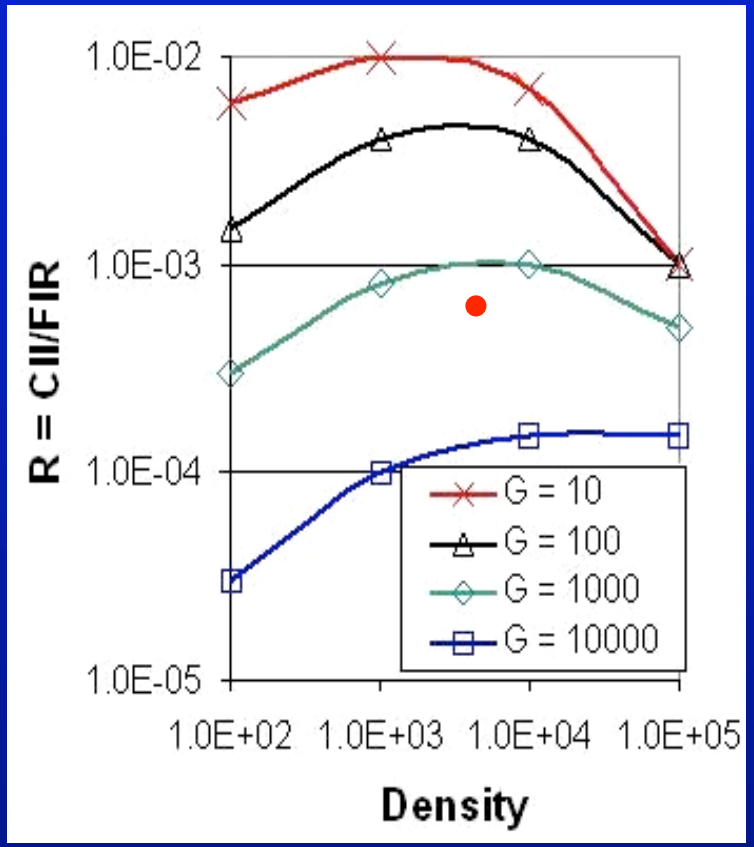

[CII]/far-IR continuum luminosity ratio vs. density for various G (from Kaufman et al).

This interesting half of the luminosity has been difficult to observe

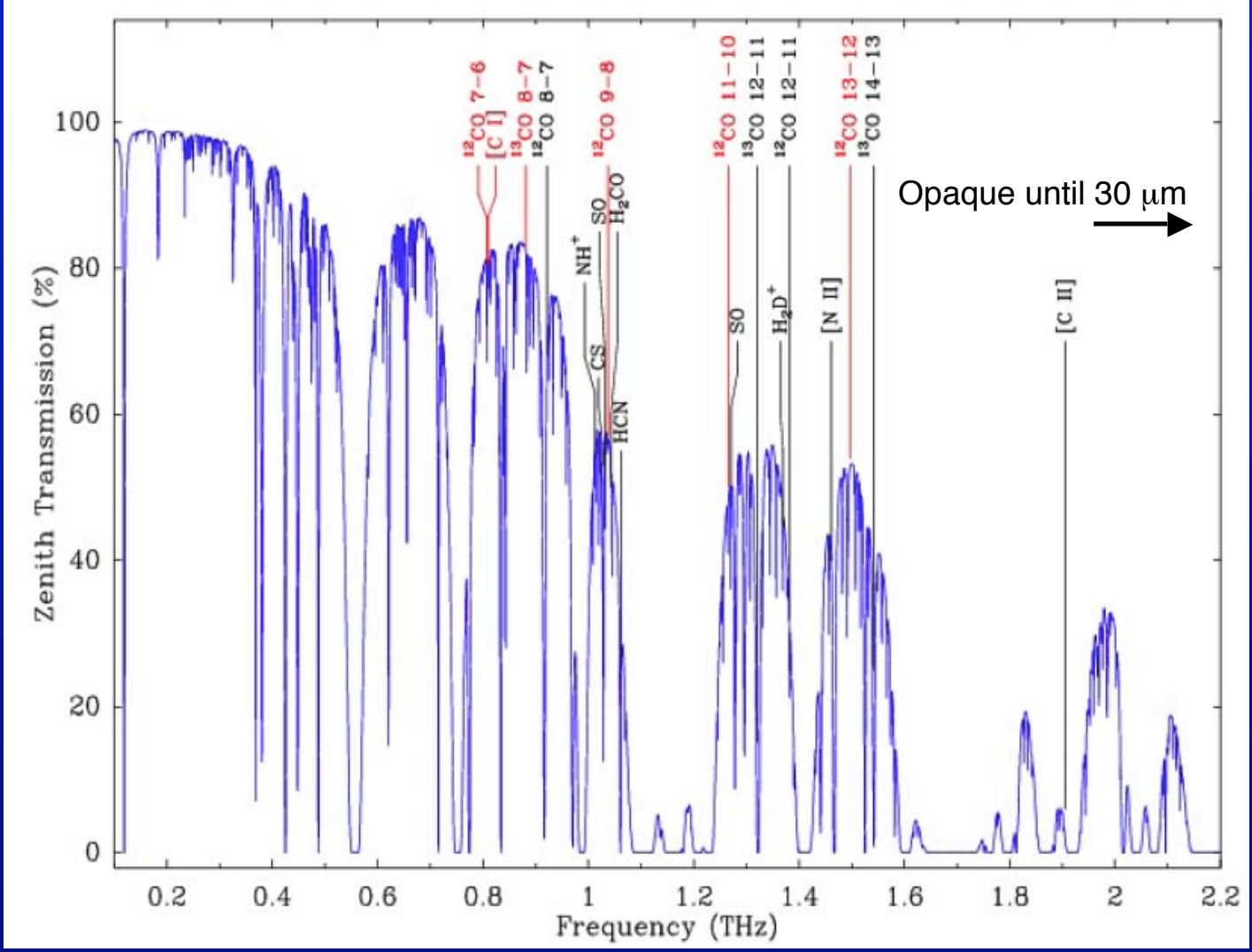

Atmosphere is opaque and warm

- Reduces transmission
- Introduces loading

-> CCAT to be at the best terrestrial site

- Far-IR /submm detector technology also behind optical / near-IR,

-> But rapidly coming of age with multi k-pix arrays

CCAT Spectrometer Telescope Requirements

- Very similar to cameras:
  - 1-2 tons of cryostat + electronics
  - 5-10 kW of electrical power
  - More modest field sizes -- few square arcmin
  - Similar data rates.
- BUT GRATING SPECTROMETER WOULD LIKE A CHOPPING SECONDARY
- Slit spectrometer needs field or instrument rotation capability
  - MOSSCCAT may be able to track sources (but not chop!)

CCAT Spectrometer Budget

- Option 1: Use modestly-upgraded Z-Spec and ZEUS
  - Labor: 10 FTE = $1.5 M,
  - Dual Z-Spec grating + detectors + electronics (NTD): $0.5 M
  - ADR + array for for ZEUS: $0.5 M
  - Total: $2.5 M for upgraded Z-Spec & ZEUS.
- Option 2: Dedicated Multi-Object CCAT Spectrometer
  - 30 kpix TES array + MUX + electronics: $6.7 M (NIST -- estimate from SW CAM camera)
  - Labor: 27 FTE: $4 M, includes spectrometer optics fabrication
  - Cryostat, pulse tube, ADR or dilution fridge: $0.5 M
  - Multi-object front end development + fabrication: $2.0 M
  - Total: $13.2 M

ULIRG evolution with redshift

From E. LeFloc'h
SPICA workshop Nov 06

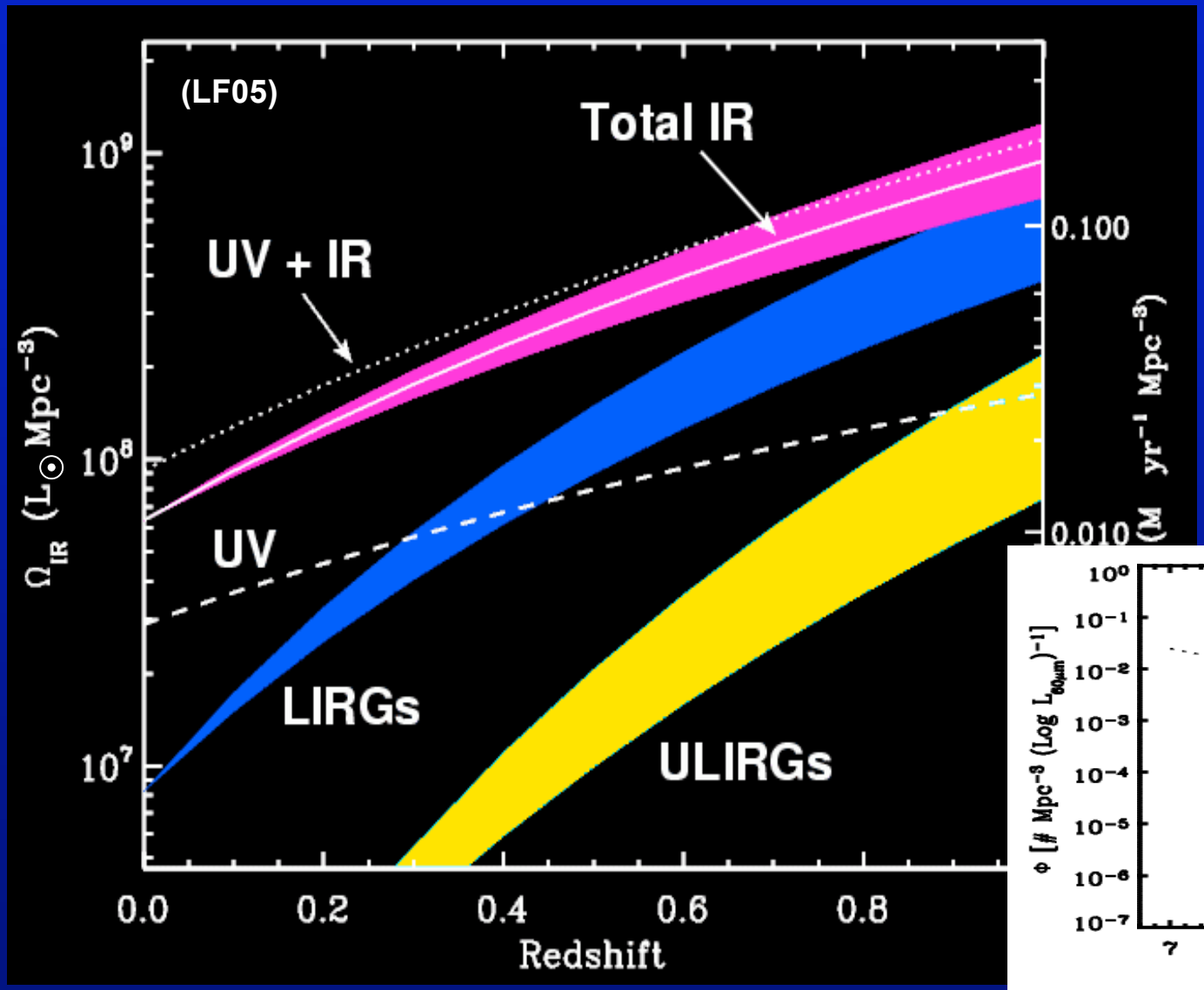

* ULIRGs are rare objects at z~0
* They underwent a strong evolution with lookback time
* They produce ~10% of the IR energy budget at z~1

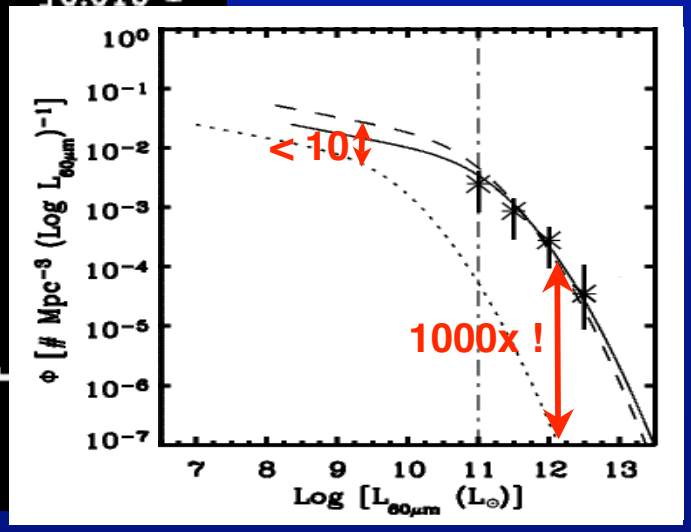

Scope of CCAT Imaging Fabry-Perot

CCAT -IFPI will be much larger than SPIFI due to the large throughput
Limitation is beam divergence in the high-res FP.

$D_{col} \sim 1.5\,\lambda\,(R \times n_{beams})^{1/2}$ so $\Omega \sim D_{col}^{4} / (1.5\,\lambda\,R)^{2}$

	R=1000			R=10000		
wavelength	array	col. Bm.	sq deg	array	spacing	d locol
220.0	256	15.2	1.31E-02	44	18.33	2.23
330.0	196	20.0	1.73E-02	20	27.50	2.26
370.0	156	20.0	1.37E-02	16	30.83	2.27
430.0	116	20.1	1.03E-02	12	35.83	2.28
490.0	90	20.1	8.02E-03	8	40.83	2.12
650.0	51	20.1	4.53E-03	5	54.17	2.23
850.0	30	20.2	2.68E-03	3	70.83	2.25
1200.0	15	20.1	1.34E-03	1.5	100.00	2.25

11' x 11' field

Will require detailed optical design

Field size driven by 20 cm beam, assumes no spatial oversampling

1-D field size for 20 cm beam

High-order FP spacing (mm) w/ F=60

Order-sorter also requires collimated 2.2cm (or slow) beam

A new R~1000 echelle spectrometer for CCAT

Design: Grating 816 micron pitch

Tilt	λ min	λ max	BW	R	slit	# pix on slit
3rd order						
58 deg	439	485	9.7%	800		
54 deg	418	462	9.3%	822	5.8	2.08
62 deg	456	504	11.0%	903		
4th order						
57 deg	330	356	7.1%	1100	4.3	1.44
63 deg	350	377	8.2%	1245		
6th order						
56.5 deg	221.3	232.7	5.0%	1646	2.7	0.96
7th order						
60.5 deg	198.7	207.4	4.3%	1920	2.7	0.96

Assuming 128 spectral element array

-- e.g. 0.86 mm pixels -- f/2.5 spectrometer, slightly oversampled

Angular deviation off the grating 18 deg total.

collimator must be oversized by 12 cm !

--> 30 cm diameter collimator

--> grating 30 cm by 40 cm, to accommodate spatial throughput

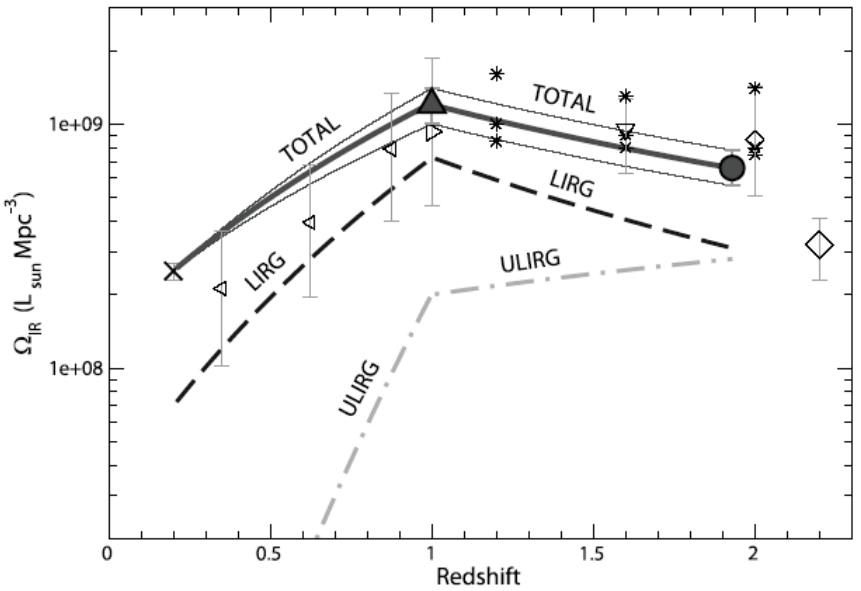

FIG. 15.—Evolution of the comoving bolometric IR luminosity density with redshift. The filled upward-pointing triangle and circle at redshifts $z = 1$ and 1.93 indicate the estimations of the respective bolometric IR luminosity density obtained in this work: $\Omega_{IR} = (1.2 \pm 0.2) \times 10^9$ and $(6.6^{+1.2}_{-1.0}) \times 10^8$ $L_\odot$ Mpc^{-3}. The density at $z = 0.2$ has been obtained from the bolometric IR LF derived from the 8 μm LF by Huang et al. (2006). The thick solid line corresponds to an interpolation between these redshifts, assuming a $[(1 + z_2)/(1 + z_1)]^x$ evolution. The thin solid lines indicate error bars on this evolution. Dashed and dot-dashed lines show the contributions of LIRGs and ULIRGs, respectively, at different redshifts. Other symbols refer to IR luminosity densities taken from the literature and based on different data sets: *ISO* mid-IR (Flores et al. 1999; *left-pointing triangles*), *Spitzer* mid-IR (Le Floc'h et al. 2005; Pérez-González et al. 2005; *right-pointing triangle and asterisks, respectively*), submillimeter (Barger et al. 2000; Chapman et al. 2005; *small and large diamonds, respectively*), and radio (Haarsma et al. 2000; *downward-pointing triangle*). Some of these IR luminosity densities have been obtained from the star formation rate densities compiled by Hopkins (2004) and converted with the Kennicutt (1998) formula $SFR = 1.72 \times 10^{-10} L_{IR}$. [*See the electronic edition of the Journal for a color version of this figure.*]